

Towards understanding epoch-wise double descent in two-layer linear neural networks

Amanda Olmin, Fredrik Lindsten
Linköping University, Sweden

Abstract

Epoch-wise double descent is the phenomenon where generalisation performance improves beyond the point of overfitting, resulting in a generalisation curve exhibiting two descents under the course of learning. Understanding the mechanisms driving this behaviour is crucial not only for understanding the generalisation behaviour of machine learning models in general, but also for employing conventional selection methods, such as the use of early stopping to mitigate overfitting. While we ultimately want to draw conclusions of more complex models, such as deep neural networks, a majority of theoretical results regarding the underlying cause of epoch-wise double descent are based on simple models, such as standard linear regression. In this paper, to take a step towards more complex models in theoretical analysis, we study epoch-wise double descent in two-layer linear neural networks. First, we derive a gradient flow for the linear two-layer model, that bridges the learning dynamics of the standard linear regression model, and the linear two-layer diagonal network with quadratic weights. Second, we identify additional factors of epoch-wise double descent emerging with the extra model layer, by deriving necessary conditions for the generalisation error to follow a double descent pattern. While epoch-wise double descent in linear regression has been attributed to differences in input variance, in the two-layer model, also the singular values of the input-output covariance matrix play an important role. This opens up for further questions regarding unidentified factors of epoch-wise double descent for truly deep models.

1 Introduction

The bias-variance trade-off implies a U-shaped generalisation error curve, as a function of model complexity. Accordingly, generalisation will improve with an increasing model complexity only to a certain point, after which the model will show signs of overfitting, and from which it never recovers. The double descent phenomenon contradicts this idea, demonstrating how generalisation performance can improve even beyond the point where the model perfectly fits the training data [6, 30], leading to a generalisation curve following a so-called double descent pattern.

The double descent pattern in generalisation error has been observed not only with respect to model size, resulting in *model-wise* double descent, but also in regards to the number of training epochs, when training models using iterative learning algorithms such as gradient descent. This type of double descent is known as *epoch-wise* double descent, see e.g. [5, 30]. While model-wise double descent has been studied extensively ([6, 1, 2, 14, 21, 13] to name a few), it typically involves understanding the asymptotic behaviour of models, assuming infinite training time. Meanwhile, epoch-wise double descent requires understanding the whole trajectory of learning.

Commonly, epoch-wise double descent has been studied either mainly through empirical observation, e.g. [30], or through the theoretical analysis of simple models, such as linear regression [22, 36, 33] or the random feature model [8, 9]. On the one end, [30] connects epoch-wise double descent, similar to model-wise double descent, to the notion of *model capacity*, attributing the second descent to the model capacity exceeding the number of training samples. On the other end, [22, 33, 9] connect epoch-wise double descent to differences in speed of learning, describing the generalisation error as consisting of overlapping bias-variance trade-off curves, corresponding to fast- and slow-learned features. With this, the eigenvalues of the input covariance matrix are integral to the double descent phenomenon. Moreover, we do not need overparametrisation for the epoch-wise double descent pattern to emerge, something that is also consistent with earlier observations of the phenomenon, see e.g. [5]. However, as the basis for these analyses are models consisting of just one layer of learnable parameters, while findings are corroborated empirically for deeper models, this leaves an open question of possibly unidentified factors causing epoch-wise double descent in deeper models.

Although [22] admittedly do also study double descent in a two-layer neural network with ReLU activation, the insights of [22] do not connect double descent in two-layer networks directly to the properties of the data, but rather to the Jacobian of the network. Meanwhile, another line of work, studying the gradient dynamics of *linear* two-layer neural networks, indicate that the singular values of the input-output covariance matrix of the training data are key factors in determining the speed of learning in these models [34, 16, 24, 37]. This suggests another possible contributor to the double descent phenomenon in two-layer linear neural networks, which has not been attributed as a factor of double descent in single-layer models. However, so far, and to the best of our knowledge, this has not been studied explicitly.

In this paper, we aim to start bridging the gap between epoch-wise double descent in the single-layer linear regression model and multi-layer neural networks, by studying double descent in the two-layer linear neural network. While this model is still linear, the training dynamics are, in contrast to the single-layer model, non-linear. Moreover, the benefits of studying linear models, is that we can obtain closed-form solutions for the training dynamics, at least in the case where weights are *decoupled*, such that they evolve independently within a transformed space that is defined by the training data. More importantly, it opens up for the possibility of directly connecting epoch-wise double

descent to properties of the training data.

For our purposes, we derive the gradient flow for a two-layer diagonal, or decoupled, neural network, similar to what was studied in [37], but with non-isotropic input, and with individual learning rates for the first and second layer. With our formulation, we can recover the standard (single-layer) linear regression model as a special case of the dynamics, and hence we can connect our findings also to this model. For the two-layer decoupled linear neural network, we then

- Derive the time-dependent generalisation error as a superposition of bias-variance curves, each corresponding to a single weight in the decoupled dynamics. The derivation is performed under the assumption that the true model is linear.
- Characterise the behaviour of the individual bias-variance trade-off curves, and use this to find a necessary condition for epoch-wise double descent.

Through this analysis, we identify additional factors of epoch-wise double descent in the two-layer model, not observed in the one-layer model, including a connection to the singular values of the input-output covariance matrix as well as an additional scenario under which epoch-wise double descent is possible.

In general, it is common to study linear shallow neural networks for gaining insights into the fundamental dynamics and behaviours of neural networks. Specifically related to the current work, are studies focusing on the learning dynamics of two-layer linear networks in gradient-based learning, apart from the ones mentioned above e.g. [35, 32, 4, 11, 26, 7, 31, 15], or the convergence of such learning algorithms, e.g. [28, 39]. Related are also studies on learning dynamics and convergence of multi-layer linear networks, see e.g. [25, 40, 29, 12].

In addition, the current work is closely connected to previous analyses of generalisation error in both linear and non-linear two-layer neural networks. This includes studies of asymptotic (in terms of the number of training epochs) generalisation error [3, 19], and of the generalisation behaviour of two-layer models trained using *one-pass* stochastic gradient descent, e.g. [18, 27, 20]. Even more relevant is [24], which derives the generalisation error for a two-layer linear network with isotropic input over the full course of learning. However, these previous works have not made direct connections to the epoch-wise double descent phenomenon. An exception is provided by [38], which establishes an upper bound on the generalisation error of two-layer neural networks based on a measure of *gradient dispersion*. This measure, in turn, empirically demonstrates connections to epoch-wise double descent. Nevertheless, [38] do not cover an explicit theoretical analysis of the phenomenon.

2 Preliminaries

We will consider the problem of predicting the target $y \in \mathbb{R}^{1 \times d_y}$ given the input $x \in \mathbb{R}^{1 \times d_x}$, using a two-layer linear network with h hidden units

$$\begin{aligned}\hat{y}(x) &= xW^\top, \\ W &= W^{(2)}W^{(1)},\end{aligned}$$

where $W^{(1)} \in \mathbb{R}^{h \times d_x}$ and $W^{(2)} \in \mathbb{R}^{d_y \times h}$.

We train the linear network on n training data points (x_i, y_i) , $i = 1, \dots, n$, using Mean Squared Error (MSE). Let

$$X = \begin{bmatrix} -x_1- \\ -x_2- \\ \dots \\ -x_n- \end{bmatrix} \in \mathbb{R}^{n \times d_x}, \quad Y = \begin{bmatrix} -y_1- \\ -y_2- \\ \dots \\ -y_n- \end{bmatrix} \in \mathbb{R}^{n \times d_y},$$

be the input and output data matrices. The MSE criterion is

$$\mathcal{L} = \frac{1}{2n} \text{Tr} \left((Y - XW^\top)^\top (Y - XW^\top) \right). \quad (1)$$

Assuming small learning rates for each model layer, $\eta_a, \eta_b \geq 0$, we study the gradient flow

$$\frac{1}{\eta_a} \frac{d}{dt} W^{(1)} = \frac{1}{n} W^{(2)\top} (Y^\top X - WX^\top X), \quad (2)$$

$$\frac{1}{\eta_b} \frac{d}{dt} W^{(2)} = \frac{1}{n} (Y^\top X - WX^\top X) W^{(1)\top}, \quad (3)$$

resulting from training the two-layer linear network using gradient descent and MSE loss.

3 Theory

In what follows, we derive decoupled dynamics for the two-layer linear neural networks, acting as a bridge between the dynamics of the one-layer linear model and the decoupled two-layer model with quadratic weights, studied in e.g. [34, 16]. Then, we use these dynamics to study factors of epoch-wise double descent in two-layer linear networks.

3.1 Decoupled dynamics of the two-layer linear network

As a first step towards understanding double descent in two-layer linear neural networks, we will study the generalisation behaviour of the decoupled dynamics considered in e.g. [34, 16, 24, 37]. While a common assumption is $X^\top X = \mathbb{I}$, i.e the input is isotropic (see e.g. [34, 24, 37]), we instead assume a non-isotropic

input where the input data matrix, X , has the singular value decomposition (SVD)

$$n^{-1/2}X = U\Lambda^{1/2}V^\top.$$

The corresponding eigendecomposition of the input covariance matrix follows according to $n^{-1}X^\top X = V\Lambda V^\top$. Relaxing the assumption of an isotropic input, allows us to evaluate the effects of the eigenvalues of this covariance matrix on the learning dynamics. Alongside this, we assume that the input-output covariance matrix $n^{-1}Y^\top X$ share right singular vectors with the input covariance matrix, and has the SVD

$$\begin{aligned} n^{-1}Y^\top X &= U^{(yx)}\Sigma V^{(yx)\top}, \\ V^{(yx)} &= V. \end{aligned}$$

Note that this assumption is similar to the one made in [16], with the exception that [16] allow for the matrix Λ to be non-diagonal, through the addition of a perturbation matrix, B . Here, we aim for simplicity and, hence, refer to [16] for results on how the perturbation matrix B might affect the final dynamics. Moreover, while our derivations should only require that the matrices V and $V^{(yx)}$ share columns, up to a reshuffling of the elements of Λ , see appendix A.1, we keep it simple by using $V^{(yx)} = V$ in the main article. We note that for the rank of $Y^\top X$ we have $\text{rank}(Y^\top X) \leq \min(\text{rank}(Y), \text{rank}(X))$, and therefore $\text{rank}(Y^\top X) \leq \text{rank}(X^\top X)$.

Following e.g. [34, 16, 24, 37] we initialise weights using a *spectral* initialisation according to $W(0) = U^{(yx)}Z(0)V^\top$, where $Z = Z^{(2)}Z^{(1)}$, and with $Z^{(1)} := W^{(1)}V$, $Z^{(2)} := U^{(yx)\top}W^{(2)}$. Then, we study the evolution of what [34] termed the *synaptic* weights $Z^{(1)}, Z^{(2)}$

$$\begin{aligned} \frac{1}{\eta_a} \frac{d}{dt} Z^{(1)} &= Z^{(2)\top}(\Sigma - Z\Lambda), \\ \frac{1}{\eta_b} \frac{d}{dt} Z^{(2)} &= (\Sigma - Z\Lambda)Z^{(1)\top}. \end{aligned} \tag{4}$$

Observe that as $U^{(yx)}$ and V are constant matrices, we will keep the relationship between W and Z throughout learning. Moreover, we follow [34, 16, 24, 37] and *decouple* weights by selecting $Z(0)$ to be diagonal. This is done by initialising the i^{th} column, $\alpha^{(i)}$, of $Z^{(1)}$, and the i^{th} row, $\beta^{(i)\top}$, of $Z^{(2)}$ according to $\alpha^{(i)}, \beta^{(i)} \propto r^{(i)}$, with $r^{(i)}$ a constant, unit vector. Importantly, $r^{(i)}$, for $i = 1, \dots, \min(d_x, d_y)$, are chosen to be orthogonal, i.e. $r^{(i)} \cdot r^{(j)} = 0$ for $i \neq j$. Decoupling weights in this manner, the rank of Z will be upper-bounded by h . In the case of an undercomplete hidden layer, i.e. $h < \min(d_x, d_y)$, this requires that we initialise some diagonal weights to 0. We initialise diagonal weight i at 0 by setting $r^{(i)}$ equal to the vector of zeroes, with $r^{(i)} = \mathbf{0}$.

With the given initialisation, Z will remain diagonal, see e.g. [34] and appendix A.1, resulting in the decoupled two layer dynamics where weights along

the diagonal evolve independently. In the decoupled dynamics, a single weight along the diagonal of Z can be described by $z_i = \alpha^{(i)} \cdot \beta^{(i)} = a_i b_i$, with scalar projections $a_i = \alpha^{(i)} \cdot r^{(i)}$, $b_i = \beta^{(i)} \cdot r^{(i)}$ evolving as

$$\begin{aligned}\frac{1}{\eta_a} \frac{da_i}{dt} &= b_i(\sigma_i - \lambda_i a_i b_i), \\ \frac{1}{\eta_b} \frac{db_i}{dt} &= a_i(\sigma_i - \lambda_i a_i b_i).\end{aligned}\quad (5)$$

We let λ_i and σ_i be the i^{th} diagonal elements of Λ and Σ , respectively. Observe that, $\lambda_i, \sigma_i \geq 0$ by definition.

To obtain a gradient flow for the product $z_i = a_i b_i$, we again follow previous work, e.g. [37], and make use of conserved quantities of the dynamical system eq. (5). Specifically, with the relaxed assumption of different learning rates, solutions to eq. (5) follow trajectories for which $\eta_b a_i^2 - \eta_a b_i^2 = \gamma_i$, where γ_i , for $i = 1, \dots, \min(d_x, d_y)$, is a constant (see appendix A.2 for the proof). Then,

$$\frac{dz_i}{dt} = \sqrt{\gamma_i^2 + 4\eta^2 z_i^2}(\sigma_i - \lambda_i z_i), \quad (6)$$

with $\eta = \sqrt{\eta_a \eta_b}$. This is an extension of the gradient flow studied in [37] with what is referred to as an asymmetric, spectral initialisation. Here, we extend the dynamics in [37] by allowing for different learning rates in the two layers as well as allowing λ_i to be different from 1. We note that, concurrent with this manuscript, [23] published a similar gradient flow to ours, using different learning rates in the two model layers. However, the gradient flow of [23] does not depend on a decoupling of the weights, and hence a solution to the dynamics is provided only in the special case $h = 1$ and $\lambda_i = 1$. Here, we provide a solution to the decoupled dynamics for general h and λ_i , although we focus on an initialisation upper bounded according to $z_i(0) < \sigma_i/\lambda_i$, which is of relevance for our later analysis.

Proposition 1 Consider $z_i(t)$ initialised at $z_i(0) < \sigma_i/\lambda_i$ and assume $\lambda_i > 0$. If $\gamma_i \neq 0$, the solution to eq. (6) is

$$z_i(t) = \frac{C^2 \lambda_i^2 \sigma_i e^{2\sqrt{\gamma_i^2 \lambda_i^2 + 4\eta^2 \sigma_i^2} t} - 2C \gamma_i^2 \lambda_i^2 e^{\sqrt{\gamma_i^2 \lambda_i^2 + 4\eta^2 \sigma_i^2} t} - 4\gamma_i^2 \eta^2 \sigma_i}{\lambda_i \left(C^2 \lambda_i^2 e^{2\sqrt{\gamma_i^2 \lambda_i^2 + 4\eta^2 \sigma_i^2} t} + 8C \eta^2 \sigma_i e^{\sqrt{\gamma_i^2 \lambda_i^2 + 4\eta^2 \sigma_i^2} t} - 4\gamma_i^2 \eta^2 \right)}, \quad (7)$$

with

$$C = \frac{\sqrt{(\gamma_i^2 \lambda_i^2 + 4\eta^2 \sigma_i^2)(\gamma_i^2 + 4\eta^2 z_i(0)^2)} + \gamma_i^2 \lambda_i + 4\eta^2 \sigma_i z_i(0)}{\lambda_i (\sigma_i - \lambda_i z_i(0))}.$$

Moreover,

$$\lim_{t \rightarrow \infty} z_i(t) = \frac{\sigma_i}{\lambda_i}. \quad (8)$$

and the weight $z_i(t)$ converges to the $z_i^* = \sigma_i \lambda_i^{-1}$ at a rate $\mathcal{O}\left(e^{-\sqrt{\gamma_i^2 \lambda_i^2 + 4\eta^2 \sigma_i^2} t}\right)$. If instead $\gamma_i = 0$, the above (eqs. (7) and (8)) holds provided that $\eta > 0$ and $z_i(0) > 0$.

We refer to appendix A.3, for the proof of proposition 1. We observe that the convergence rate is dependent on both the eigenvalue λ_i and the singular value σ_i , where the parameters γ_i, η control their respective influence. For a large absolute value of the conservation quantity γ_i (also referred to as the level of initialisation imbalance, see e.g. [37]), relative to the parameter η , the eigenvalue λ_i of the input covariance matrix will dominate the rate of convergence. If instead the learning rate parameter η is large, relative to $|\gamma_i|$, the singular value σ_i of the input-output covariance matrix will dominate this rate.

Throughout the paper, we will pay special attention to two special cases of the dynamics. The first special case is $\eta_a = 0$ ($\eta = 0$), which corresponds to fixed first layer weights, resulting in the dynamics of the standard linear regression model, see e.g. [16], with solution

$$z_i(t) = e^{-|\gamma_i| \lambda_i t} (z_i(0) - \sigma_i \lambda_i^{-1}) + \sigma_i \lambda_i^{-1}. \quad (9)$$

We will sometimes also refer to the linear regression model as the *one-layer* model. Importantly, since we recover the one-layer model as a special case of the decoupled dynamics, we will be able to connect our findings to previous results on epoch-wise double descent for this model, e.g. [22, 33].

The second special case is $\gamma_i = 0$, for which we recover the *balanced* dynamics, studied in e.g. [34, 16], with solution

$$z_i(t) = \frac{\sigma_i e^{2\eta \sigma_i t} z_i(0)}{\lambda_i (e^{2\eta \sigma_i t} - 1) z_i(0) + \sigma_i}. \quad (10)$$

We observe that the two special cases represents boundary cases of the general solution, in the sense that for $\eta = 0$, the time-dependent exponential term depends only on the eigenvalue value λ_i , and not on σ_i , while for $\gamma_i = 0$, the time dependent exponential term instead depends only on σ_i , and not on λ_i .

We note that under eq. (6), weights $z_i(t)$ that are initialised at 0, by initialising $a_i(0) = b_i(0) = 0$ (resulting in $\gamma_i = 0$), will remain at 0. Hence, depending on the initialisation, only a subset of the diagonal elements of $Z(t)$ will change during the course of learning. We will refer to these non-constant weights as *active* and use $S_A \subseteq \{1, 2, \dots, \min(d_x, d_y)\}$ with size $|S_A|$ to denote the set of indices corresponding to active weights in $Z(t)$.

3.2 Epoch-wise double descent in the two-layer model

We study the generalisation dynamics of Z , when weights are learned following the decoupled dynamics in eq. (6). First, for deriving the test MSE, we will assume that x is Gaussian with mean zero and true covariance matrix $\bar{\Lambda}$, written as $x \sim \mathcal{N}(\mathbf{0}, \bar{\Lambda})$. In addition, we assume that y follows a linear model

$$y = x \bar{W}^\top + \epsilon, \quad (11)$$

with true weights $\bar{W} \in \mathbb{R}^{d_y \times d_x}$. The noise parameter, $\epsilon \in \mathbb{R}^{1 \times d_y}$, is assumed to be zero-mean Gaussian with covariance matrix $\Lambda^{(\epsilon)}$, i.e. $\epsilon \sim \mathcal{N}(\mathbf{0}, \Lambda^{(\epsilon)})$. In the synaptic weight space, the true weights are

$$\bar{Z} := U^{(yx)\top} \bar{W} V. \quad (12)$$

We provide an alternative formulation of \bar{Z} in the following lemma.

Lemma 1 *Assume that elements of the output data matrix, Y , follow the linear model given in eq. (11) and let*

$$E = \begin{bmatrix} -\epsilon_1 - \\ -\epsilon_2 - \\ \dots \\ -\epsilon_n - \end{bmatrix},$$

be the matrix of residual vectors $\epsilon_i = y_i - x_i \bar{W}^\top$, for $i = 1, \dots, n$. The true synaptic weight matrix, given in eq. (12), can be rewritten according to

$$\begin{aligned} \bar{Z} &= \Sigma \Lambda^\dagger - \tilde{E}^\top (\Lambda^{1/2})^\dagger, \\ \tilde{E} &:= n^{-1/2} U^{(yx)\top} E U, \end{aligned}$$

with \dagger denoting the Moore-Penrose pseudoinverse.

Subsequently, the i^{th} diagonal element of \bar{Z} , assuming that $\lambda_i > 0$, can be expressed as

$$\bar{z}_i = \sigma_i \lambda_i^{-1} - \tilde{\epsilon}_i \lambda_i^{-1/2}. \quad (13)$$

where we let $\tilde{\epsilon}_i$ denote the i^{th} element on the main diagonal of \tilde{E} .

For the purpose of studying epoch-wise double descent, we use lemma 1 to derive a time-dependent expression for the generalisation error of the decoupled two-layer linear network.

Proposition 2 *Consider the diagonal weight matrix $Z(t)$ with weights $z_i(t)$ on the diagonal following the decoupled dynamics in eq. (6). Moreover, assume $x \sim \mathcal{N}(\mathbf{0}, \bar{\Lambda})$ and that y follows the linear model given by eq. (11). Then, using MSE as the error metric and approximating $\bar{\Lambda} \approx V \Lambda V^\top$, the total generalisation error of $Z(t)$ can be written as a sum of $|S_A|$ individual error curves, according to*

$$\begin{aligned} \mathcal{L}_G(t) &= \frac{1}{2} \mathbb{E}_{x,y} \left[(y - xW(t)^\top)(y - xW(t)^\top)^\top \right] \\ &\approx \frac{1}{2} \sum_{i \in S_A} \lambda_i (\bar{z}_i - z_i(t))^2 + \text{const.} \end{aligned} \quad (14)$$

The true weights, \bar{z}_i , are given by lemma 1. Each individual error term within the sum in eq. (14) is either monotonically decreasing, U-shaped, or monotonically increasing, and, hence, the total generalisation error is a sum of such curves.

Following proposition 2, the total generalisation error of $Z(t)$ is described by $|S_{\mathcal{A}}|$ overlapping error curves. Depending on the initialisation, the test MSE might include additional constant error, covering error corresponding to inactive diagonal elements, i.e., $z_i(t)$ for which $i \notin S_{\mathcal{A}}$. Constant error can also arise from assuming that the weight matrix, $Z(t)$, is diagonal, while the true weight \bar{Z} may not be. Moreover, we bring attention to the fact that eq. (14) relies on the assumption that the training sample size is large enough for the sample covariance matrix, $V\Sigma V^{\top}$, to approximate the true covariance matrix, $\bar{\Lambda}$ (i.e. $\bar{\Lambda} \approx V\Lambda V^{\top}$). Proofs for both lemma 1 and proposition 2 are provided in appendix A.4.

We acknowledge that similar expressions for the generalisation error, as given by proposition 2, have been provided previously. In comparison with [24], we consider the more general decoupled dynamics given by eq. (6), while [24] consider the balanced dynamics as well as an isotropic input, i.e. $\lambda_i = 1$ and $\gamma_i = 0 \forall i \in [1, \dots, \min(d_x, d_y)]$. In this context, we also mention [22] that determines a time-dependent upper bound on the test MSE of a two-layer neural network with ReLU activation. According to [22], this upper bound is broadly interpreted as a sum over n bias-variance trade-off curves. Moreover, the general expression in eq. (14), without making assumptions regarding the dynamics of the diagonal weights $z_i(t)$, naturally also shares similarities with corresponding expressions derived for the one-layer and random feature models when training with (stochastic) gradient descent, see e.g. [2, 22, 33, 10].

Indeed, for the decoupled two-layer neural network, we uncover additional commonalities with the one-layer model. Namely, with each diagonal weight $z_i(t)$ following the decoupled two-layer dynamics in eq. (6), we find that a single curve in the sum of eq. (14) will not, by itself, exhibit a double descent pattern. Therefore, and equivalent to what was found for the one-layer model in [22], epoch-wise double descent in the decoupled linear two-layer model, must be a result of overlapping error curves. Moreover, each such error curve corresponds to the error of a single weight, $z_i(t)$. The latter is in contrast to what [22] concludes for the non-linear two-layer model, where the bias-variance curves in the upper bound corresponds to dimensions of the network Jacobian.

3.2.1 Analysis of error curves

To understand which factors give rise to the double descent behaviour, we start by analysing the individual error curves in eq. (14). First, observe that the initialisation $z_i(0)$ as well as the position of the true minimum \bar{z}_i relative to $z_i(0)$ and the global minimum z_i^* , will determine the behaviour of $z_i(t)$, as well as the shape of its error curve. For example, if $z_i(0) > \sigma_i/\lambda_i$, $z_i(t)$ will decrease in t , while for the opposite ($z_i(0) < \sigma_i/\lambda_i$), $z_i(t)$ will increase in t . Moreover, if \bar{z}_i does not lie on the path between the initialisation $z_i(0)$ and the global minimum z_i^* , then $z_i(t)$ will never pass this point and so, the corresponding error curve will be either monotonically decreasing or monotonically increasing in t .

To limit the number of possible scenarios, we will restrict our analysis to

the case where $z_i(t)$ is positive and increasing in t . In addition, we will assume that $\bar{z} \in [0, z_i^*]$, noting that this also covers cases where the error curve of $z_i(t)$ is monotonically increasing/decreasing in t , albeit with a focus on what we presume to be the most interesting scenario; the one where $\bar{z}_i \in [z_i(0), z_i^*]$, such that the error curve for $z_i(t)$ is U-shaped. Hence, for our further analysis, we will assume that the following two conditions hold for each $i \in S_{\mathcal{A}}$:

- (i) The model weight $z_i(t)$ is initialised with $z_i(0) \in [0, \bar{z}_i]$.
- (ii) The true minimum \bar{z}_i lies in the interval $[0, z_i^*]$, such that it can be reparameterised as $\bar{z}_i = (1 - \rho_i)z_i^*$, where ρ_i is a constant in the interval $[0, 1]$.

Condition (i) ensures that each active weight $z_i(t)$ is increasing in t and remains positive throughout training. Except for initialising $z_i(t) \geq 0$, we put an upper bound $\bar{z}_i \geq z_i(0)$, such that the weight $z_i(t)$ is initialised before or at the true minimum, \bar{z}_i . Meanwhile, condition (ii) restricts \bar{z}_i to lie on the path between 0 and z_i^* . With this restriction, we put a focus on the scenarios where the error curve for $z_i(t)$ is U-shaped, while still including scenarios where the error curve is monotonically decreasing in t ($\rho_i = 0$) as well as monotonically increasing in t ($1 \geq \rho_i \geq 1 - z_i(0)/z_i^*$). We emphasise that the purpose of conditions (i)-(ii) is to make the analysis more concise by limiting the number of possible scenarios to be considered in our analysis of epoch-wise double descent. By similar arguments as used in the following analysis, the results are believed to be extendable beyond these conditions.

Since inactive weights will not contribute to the dynamics of the generalisation error, we focus on active weights, i.e. $z_i(t)$ for which $i \in S_{\mathcal{A}}$. Under conditions (i)-(ii), the following additional conditions must be fulfilled for a weight $z_i(t)$ to be active:

- (iii) As additions to condition (i):
 - If $\gamma_i = 0$, then $z_i(0) \in (0, \bar{z}_i]$.
 - If $\bar{z}_i = z_i^*$ ($\rho_i = 0$), then $z_i(0) \in [0, \bar{z}_i)$.
- (iv) The i^{th} singular value of $n^{-1}Y^\top X$ is non-zero, i.e. $\sigma_i > 0$.
- (v) If $\eta = 0$, the learning rates η_a, η_b and the initialisation of $z_i(t)$ are chosen such that $\gamma_i \neq 0$. Similarly, if $\gamma_i = 0$, then the learning rates η_a, η_b are chosen such that $\eta > 0$.

Any diagonal weight $z_i(t)$ fulfilling conditions (i)-(ii), but not all of the conditions (iii)-(v) will be inactive, as either the weight is initialised at a fixed point, where it will remain, or the *effective* learning rate $\sqrt{\gamma_i^2 \lambda_i^2 + 4\eta^2 \sigma_i^2}$ is 0. Notice that, since $\text{rank}(Y^\top X) \leq \text{rank}(X^\top X)$, condition (iv) implies $\lambda_i > 0, \forall i \in S_{\mathcal{A}}$, and that proposition 1 therefore holds under conditions (i)-(v).

Using condition (ii) and the reparametrisation of \bar{z}_i in terms of the parameter ρ_i , we rewrite a single error term in the sum of eq. (14) as

$$\mathcal{L}_{\mathcal{G},i}(t) = ((1 - \rho_i)\sigma_i - \lambda_i z_i(t))^2. \quad (15)$$

The parameter ρ_i determines the relative position of the true minimum, \bar{z}_i , to the initialisation $z_i(0)$ as well as the global minimum z_i^* , and hence the form of the generalisation curve. As part of the following analysis, we will consider the time it takes for $z_i(t)$ to reach this true minimum, starting at $z_i(0)$. Under conditions (i)-(v) this time, denoted $t_i^{(1-\rho_i)z_i^*}$, can be expressed according to

$$t_i^{(1-\rho_i)z_i^*} = \frac{\log \left(\frac{\sqrt{(\gamma_i^2 \lambda_i^2 + 4\eta^2 \sigma_i^2)(\gamma_i^2 \lambda_i^2 + 4\eta^2 \sigma_i^2(1-\rho_i)^2)} + \gamma_i^2 \lambda_i^2 + 4\eta^2 \sigma_i(1-\rho_i)}{C \lambda_i^2 \sigma_i \rho_i} \right)}{\sqrt{\gamma_i^2 \lambda_i^2 + 4\eta^2 \sigma_i^2}}, \quad (16)$$

with the constant C defined in proposition 1. See appendix A.3 for the derivation.

Starting from eq. (15), we provide the following two lemmas characterising the behaviour of the error curve $\mathcal{L}_{G,i}(t)$.

Lemma 2 *Consider the weight $z_i(t)$ following the dynamics in eq. (6), under conditions (i)-(v). If $1 \geq \rho_i > 0$, the generalisation curve of $z_i(t)$, eq. (15), is convex in t at \bar{z}_i . If instead $\rho_i = 0$, the curve is convex leading up to the point \bar{z}_i , while \bar{z}_i itself is an undulation point.*

Lemma 3 *Consider the weight $z_i(t)$ following the dynamics in eq. (6). Under conditions (i)-(v), the generalisation curve for $z_i(t)$, eq. (15), has a maximum of three inflection points on the interval $[0, \infty)$, whereof a maximum of two lies in the interval $(0, t_i^{(1-\rho_i)z_i^*})$. Moreover, in the case that three inflection points exist and if $5/7 > \rho_i > 0$, then exactly two inflection points lie in the interval $(0, t_i^{(1-\rho_i)z_i^*})$ and one in the interval $(t_i^{(1-\rho_i)z_i^*}, \infty)$.*

We leave the proof of lemmas 2 and 3 to appendices A.5 and A.6. We highlight the following special cases of lemma 3:

- **One-layer dynamics ($\eta = 0$)**. For $1 \geq \rho_i > 0$, the error curve has one inflection point

$$\hat{t}_i^+ = \frac{\log \left(\frac{2(\sigma_i - \lambda_i z_i(0))}{\sigma_i \rho_i} \right)}{|\gamma_i| \lambda_i} \quad (17)$$

lying in the interval $(t_i^{(1-\rho_i)z_i^*}, \infty)$. For $\rho_i = 0$, the curve has no inflection points.

- **Balanced two-layer dynamics ($\gamma_i = 0$)**. For $1 > \rho_i > 0$, the error curve has up to two inflection points

$$\hat{t}_i^\pm = \frac{\log \left(\frac{(\sigma_i - \lambda_i z_i(0))(1 \pm \sqrt{\rho_i^2 - \rho_i + 1})}{\lambda_i \rho_i z_i(0)} \right)}{2\eta \sigma_i}, \quad (18)$$

one, if it exists, lying in the interval $(0, t_i^{(1-\rho_i)z_i^*})$ and one in the interval $(t_i^{(1-\rho_i)z_i^*}, \infty)$. If $\rho_i = 0$, the curve has one potential inflection point

$$\hat{t}_i^- = \frac{\log \left(\frac{\sigma_i - \lambda_i z_i(0)}{2\lambda_i z_i(0)} \right)}{2\eta\sigma_i},$$

if it exists, lying in the interval $(0, t_i^{(1-\rho_i)z_i^*})$. In other words, for the balanced dynamics, the curve has up to two inflection points for $1 > \rho_i > 0$, lying on either side of $t_i^{(1-\rho_i)z_i^*}$, but only one inflection point if $\rho_i = 0$. For \hat{t}^- to exist, we require $z_i(\hat{t}^-) \in (z_i(0), \bar{z}_i)$.

Lemmas 2 and 3 tell us something about the general form of each individual error curve $\mathcal{L}_{\mathcal{G},i}(t)$, $i \in S_{\mathcal{A}}$, as given by eq. (15). We observe that under the one-layer model ($\eta = 0$), the error curve $\mathcal{L}_{\mathcal{G},i}(t)$ has a maximum of one inflection point, with the curve being convex to start, and potentially becoming concave at a time point after $t_i^{(1-\rho_i)z_i^*}$. On the other hand, the error curve under the decoupled two-layer model can have up to three inflection points. With this, the error curve is potentially concave on parts of the time interval $[0, t_i^{(1-\rho_i)z_i^*})$. For the balanced dynamics, for example, the curve can, depending on the initialisation, be concave to begin with, consistent with the initial plateau in learning previously observed for two-layer linear networks with small initialisation [2].

We will consistently use \hat{t}_i^- to denote the *maximum* inflection point of the error curve $\mathcal{L}_{\mathcal{G},i}(t)$ located in the interval $(0, t_i^{(1-\rho_i)z_i^*})$ and \hat{t}_i^+ the *minimum* inflection point located in the interval $(t_i^{(1-\rho_i)z_i^*}, \infty)$. In other words, provided that they exist, \hat{t}_i^- and \hat{t}_i^+ are the two inflection points located closest to, and on either side of, the minimum of $\mathcal{L}_{\mathcal{G},i}(t)$. Following lemma 2, the error curve is convex in between these points. We will use this to understand under which conditions epoch-wise double descent may occur.

3.2.2 Necessary condition for epoch-wise double descent

We have analysed the behaviour of the individual error curves of the total generalisation error in eq. (14). Following the conclusion that epoch-wise double descent in the decoupled two-layer model emerges in the superposition of such curves, we use our insights to find a necessary condition for epoch-wise double descent.

Proposition 3 *Consider the weight matrix $Z(t)$ with $|S_{\mathcal{A}}|$ active weights, following eq. (6). The total generalisation error, eq. (14), is a sum of $|S_{\mathcal{A}}|$ error curves. Under conditions (i)-(v), a necessary condition for this generalisation error to exhibit a double descent pattern over the course of learning, is that we can find at least one inflection point, \hat{t} , belonging to either one of the $|S_{\mathcal{A}}|$ individual error curves, such that*

$$\min\{t_i^{(1-\rho_i)z_i^*}; i \in S_{\mathcal{A}}\} < \hat{t} < \max\{t_i^{(1-\rho_i)z_i^*}; i \in S_{\mathcal{A}}\}.$$

Proposition 3 gives a necessary, but not sufficient, condition for epoch-wise double descent in the case of a general number of active weights $|S_{\mathcal{A}}|$. For brevity, we will study this condition further in the case of two active weights, $z_i(t)$ and $z_j(t)$.

Corollary 1 *Consider the weight matrix $Z(t)$ with two active weights, $z_i(t)$ and $z_j(t)$, following eq. (6) and for which, without loss of generality, $t_i^{(1-\rho_i)z_i^*} < t_j^{(1-\rho_j)z_j^*}$. The total generalisation error, eq. (14), is a sum of two error curves. Under conditions (i)-(v), a necessary condition for this generalisation error to exhibit a double descent pattern over the course of learning, is that we can find at least one inflection point, \hat{t} , belonging to either one of the two individual error curves, such that*

$$t_i^{(1-\rho_i)z_i^*} < \hat{t} < t_j^{(1-\rho_j)z_j^*}.$$

Moreover, provided that they exist, let \hat{t}_j^- denote the maximum inflection point of the error curve belonging to $z_j(t)$, and lying on the interval $(0, t_j^{(1-\rho_j)z_j^*})$ and let \hat{t}_i^+ denote the minimum inflection point belonging to the error curve of $z_i(t)$ and lying on the interval $(t_i^{(1-\rho_i)z_i^*}, \infty)$. The necessary condition for epoch-wise double descent simplifies to fulfilling one of the following two conditions

$$\begin{aligned} t_i^{(1-\rho_i)z_i^*} &< \hat{t}_j^-, \\ \hat{t}_i^+ &< t_j^{(1-\rho_j)z_j^*}. \end{aligned}$$

From corollary 1, we observe that when Z has two active weights, $z_i(t)$ and $z_j(t)$, epoch-wise double descent can happen in one of two scenarios. From an intuitive perspective, we might interpret the first scenario, $t_i^{(1-\rho_i)z_i^*} < \hat{t}_j^-$, as one where learning of the first weight, $z_i(t)$, tapers off at a point where the generalisation error of the second weight, $z_j(t)$, is still improving. Perhaps particularly so in the case $5/7 > \rho_i > 0$, where the minimum inflection point \hat{t}_i^+ is the only inflection point of $\mathcal{L}_{\mathcal{G},i}(t)$ located after $t_i^{(1-\rho_i)z_i^*}$ (see lemma 2). Similarly, we might interpret the second scenario, $\hat{t}_i^+ < t_j^{(1-\rho_j)z_j^*}$, as one where learning of the second weight, $z_j(t)$, starts to progress first after the first weight, $z_i(t)$, shows signs of overfitting. We refer to appendix A.7 for the proofs of proposition 3 and corollary 1.

Interestingly, we find that, while the necessary condition for epoch-wise double descent under the balanced dynamics, and with two active weights, also includes two scenarios in which double descent can occur, we find that the same necessary condition under the one-layer model only includes one of the two scenarios:

- **One-layer dynamics ($\eta = 0$).** For $1 \geq \rho_i > 0$, let \hat{t}_i be the inflection point of the error curve corresponding to the weight $z_i(t)$, given by eq. (17).

Then, the necessary condition for epoch-wise double descent with two active weights, given in corollary 1, simplifies to

$$\hat{t}_i < t_j^{(1-\rho_j)z_j^*}.$$

If $z_i(0) = z_j(0) = 0$ and $\gamma_i = \gamma_j$, this condition is equivalent to

$$\log\left(\frac{2}{\rho_i}\right) \leq \frac{\lambda_i}{\lambda_j} \log\left(\frac{1}{\rho_j}\right).$$

Thereby, we obtain a necessary condition for epoch-wise double descent under the one-layer model, that depends on the eigenvalues λ_i, λ_j of the input covariance matrix, but not the singular values σ_i, σ_j . Note that for $\rho_i = 0$, and when $\eta = 0$, there is no inflection point \hat{t} fulfilling the necessary condition of corollary 1.

- **Balanced two-layer dynamics ($\gamma_i = 0 \forall i \in S_{\mathcal{A}}$).** In the case of the balanced two-layer dynamics, let \hat{t}_j^-, \hat{t}_i^+ be the inflection points given by eq. (18), for the error curves corresponding to the weights $z_j(t), z_i(t)$, respectively. The necessary condition for epoch-wise double descent with two active weights, given in corollary 1, corresponds to fulfilling at least one of the following two conditions:

(i) For $1 > \rho_j \geq 0$

$$t_i^{(1-\rho_i)z_i^*} < \hat{t}_j^-,$$

(ii) For $1 > \rho_i > 0$

$$\hat{t}_i^+ < t_j^{(1-\rho_j)z_j^*}.$$

Observe that the second condition is not possible for $\rho_i = 0$.

First, we notice that epoch-wise double descent with two active weights, can not happen if $\rho_i = 0$, where the error curve belonging to $z_i(t)$ is monotonically decreasing. This is also true in the general case, as for $\rho_i = 0$, we have $t_i^{(1-\rho_i)z_i^*} = t_i^{z_i^*} = \infty$. Similarly, double descent can not occur if $\rho_j = 1$, where the error curve belonging to $z_j(t)$ is monotonically increasing, as for $\rho_j = 1$, we have $t_j^{(1-\rho_j)z_j^*} = t_j^0 = 0$.

More importantly, and as mentioned previously, there is only one scenario where epoch-wise double descent can happen in the one-layer model; namely the scenario where learning of the first weight, $z_i(t)$, starts to taper off at a point where the generalisation error of the second weight, $z_j(t)$, is still improving. Meanwhile, the necessary condition for epoch-wise double descent in the case $\gamma_i = 0 \forall i \in S_{\mathcal{A}}$, i.e. the balanced dynamics, include the same two scenarios

as in the general case, given by corollary 1, but where t_j^-, t_j^+ are the only two inflection points that can lie in the interval $(t_i^{(1-\rho_i)z_i^*}, t_j^{(1-\rho_j)z_j^*})$.

Furthermore, for vanishing initialisation, we obtain a necessary condition for epoch-wise double descent in the one-layer model that is independent of the singular values of the input-output covariance matrix. This is in accordance with previous observations where only the eigenvalues $\lambda_i, i \in S_{\mathcal{A}}$, and not the singular values $\sigma_i, i \in S_{\mathcal{A}}$, have been identified as factors of epoch-wise double descent, attributing double descent to input features being learned at different speeds, see e.g. [22, 33, 9].

In simulations, as shown in fig. 1, we also do not observe a relationship between epoch-wise double descent and the singular values $\sigma_i, i \in S_{\mathcal{A}}$, for the one-layer model, while we do observe such a dependence for the two-layer model (bottom row of fig. 1). Considering the balanced two-layer model, $\gamma_i = 0 \forall i \in S_{\mathcal{A}}$, our findings are in accordance with observations made by e.g. [16], where the singular values $\sigma_i, i \in S_{\mathcal{A}}$, determines the learning speed at vanishing initialisation, although these observations have not been connected to epoch-wise double descent. Moreover, the findings align with proposition 1, where the singular values of the input-output covariance matrix have an effect on the convergence rate of the weight $z_i(t)$ only when $\eta > 0$. Although, here we do find that also the eigenvalues $\lambda_i, i \in S_{\mathcal{A}}$, can impact epoch-wise double descent in the case $\gamma_i = 0 \forall i \in S_{\mathcal{A}}$, which is not indicated by this convergence rate.

In practice, we find that for large differences between eigenvalues (λ_i and λ_j) or singular values (σ_i and σ_j), one error curve tends to dominate the sum of eq. (14), and thereby the double descent pattern is concealed. For the simulations in fig. 1, we therefore mimic the scenario where several weights have either large eigenvalues or small singular values, by duplicating one of the weights $z_i(t)$ and $z_j(t)$.

Apart from the eigenvalues $\lambda_i, i \in S_{\mathcal{A}}$ as well as the singular values $\sigma_i, i \in S_{\mathcal{A}}$, another factor that could potentially cause double descent, are relative distances to the true weights $\bar{z}_i, i \in S_{\mathcal{A}}$ in the different dimensions, depending on the parameter ρ_i . The true noise model will indeed have an effect on double descent also in the single-layer model, see e.g. [36]. Moreover, differences in initialisation and learning rates, could also be factors affecting the form of the generalisation curve in eq. (14), including the potential emergence of a double descent pattern.

4 Discussion

We investigate epoch-wise double descent in decoupled two-layer linear networks, identifying factors of epoch-wise double descent in gradient-based learning. First, apart from differences in the eigenvalues of the input covariance matrix of the training data, also differences in the singular values of the input-output covariance matrix can cause epoch-wise double descent in the two-layer model. Second, by providing a necessary condition for epoch-wise double descent both for the standard linear regression model and for the linear decoupled two-layer network, we reveal an additional circumstance under which epoch-

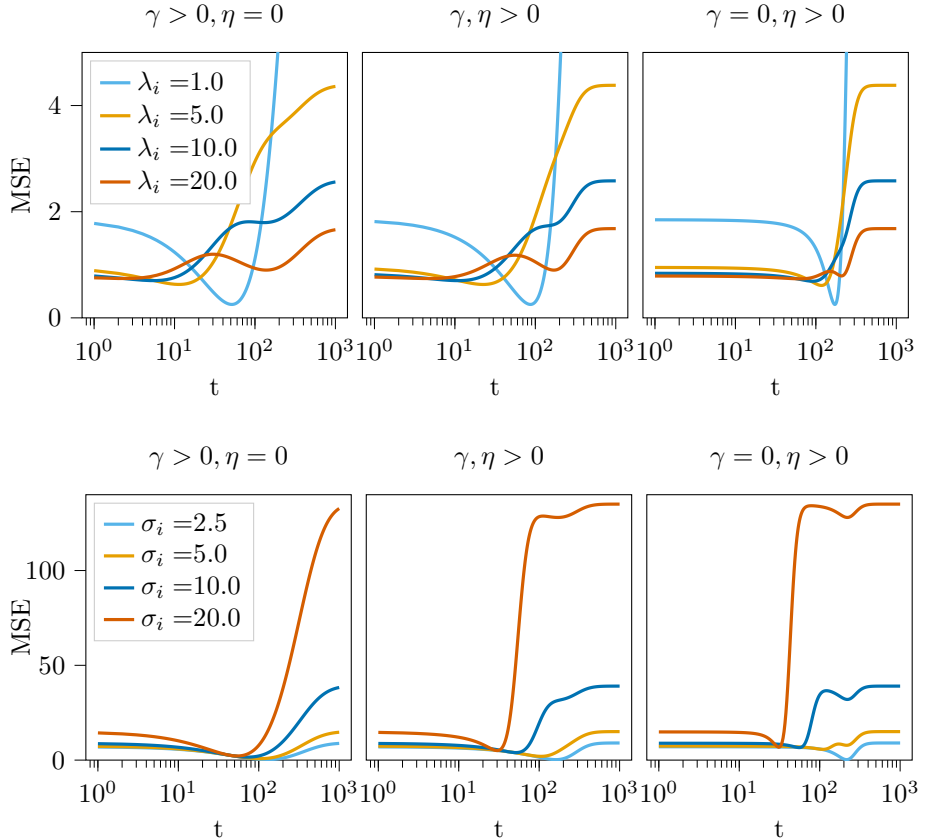


Figure 1: Examples of double descent with $|S_{\mathcal{A}}| = 10$ active weights, and where active weights are divided into two sets; one set evolving as $z_i(t)$ and the other as $z_j(t)$. We let $\gamma_i = \gamma_j = \gamma$ and consider three scenarios with different values of the parameters γ, η (Left: one-layer dynamics with $\gamma = 0.005, \eta = 0$. Middle: bridged dynamics with $\gamma = 0.0025, \eta = 0.0025$. Right: balanced dynamics with $\gamma = 0, \eta = 0.005$.). As default, remaining parameters are set according to $\lambda_i = \lambda_j = 1.0, \sigma_i = \sigma_j = 2.5, \rho_i = 0.5, \rho_j = 0.8$ and $z_i(0) = z_j(0) = 0.01$. **Top:** Changing λ_i . The weight $z_i(t)$ has multiplicity 9, while $z_j(t)$ has multiplicity 1. We observe double descent for large λ_i in all three scenarios, but double descent seems to appear for a smaller λ_i when γ is larger. **Bottom:** Changing σ_i . The weight $z_i(t)$ has multiplicity 1, while $z_j(t)$ has multiplicity 9. We observe double descent for large σ_i only in the scenarios where $\eta > 0$.

wise double descent can emerge in the two-layer model, not observed for the one-layer model.

There are several venues for further investigating epoch-wise double descent in (linear) neural networks, with the aim to better understand the causes of epoch-wise double descent in deep models. For one, it remains to be investigated if patterns in the training loss, such as the previously observed incremental learning pattern, see e.g [16, 17, 7], could be indicators of epoch-wise double descent. Moreover, several assumptions were made leading up to the dynamics in eq. (6) and relaxing these assumptions could render new insights into the epoch-wise double descent phenomenon. We shortly discuss two extensions, namely that of deep(er) linear neural networks, as well as that of studying the dynamics of eq. (4) without decoupling of the weights.

Incremental learning and epoch-wise double descent Integral to understanding learning dynamics is the training loss, eq. (1). Previous studies on two-layer linear neural networks have discovered an implicit bias of gradient descent, causing an incremental learning pattern where weights are learned sequentially and where the training loss typically exhibits plateaus of close to constant error, see e.g. [17, 16, 7]. It would be an interesting venue to investigate whether incremental learning, bearing similarities with the epoch-wise double descent phenomenon, could be an indicator of epoch-wise double descent.

Deeper models While both the standard linear regression model and the two-layer linear neural network are indeed linear models, we have seen that they exhibit different learning behaviours. Hence, as the number of layers, L , grows, we might expect the dynamics to change further. Let us consider the linear neural network with L layers, where the weight matrix in the synaptic weight space can be described as

$$Z = U^{(yx)^\top} W V = \prod_{\ell=1}^L Z^{(\ell)},$$

each layer ℓ represented by the weight matrix $Z^{(\ell)}$ and with its own number of hidden units. Similar to the two-layer model, we can decouple the weights of $Z(t)$, such that they evolve independently. Then, to obtain an approximate dynamics for the i^{th} diagonal element, $z_i(t)$, of $Z(t)$, we make a number of simplifications, including assuming L to be even and large as well as grouping the model layers into two groups of equal learning rates and initialisation. The approximate dynamics are

$$\frac{dz_i}{dt} \approx \frac{L}{2} |\gamma_i| z_i^2 (\sigma_i - \lambda_i z_i). \quad (19)$$

We refer to appendix A.8 for the derivation. The dynamics in eq. (19) are similar to the dynamics of multi-layer linear neural networks found in [34], but with a weight γ_i and λ_i possibly different from 1. The parameter γ_i is a conservation

quantity, similar to the same parameter in eq. (6). In the approximate L -layer dynamics, this parameter has a direct influence on the size of the gradient. Meanwhile the counterpart of the learning rate parameter, η , in the two-layer dynamics, vanishes as L grows large, although the learning rates of the layers still have an implicit effect on the learning dynamics through γ_i .

We observe that the dynamics in eq. (19) are cubic in $z_i(t)$. However, under the simplified assumptions made here, together with conditions (i)-(v) and provided that $\gamma_i \neq 0$ and $z_i(0) \neq 0$, the error curve $\mathcal{L}_{G,i}(t)$ (eq. (15)) will be monotonically decreasing, U-shaped, or monotonically increasing in t , just as the corresponding error curve under the decoupled two-layer dynamics, see appendix A.8. Moreover, the error curve $\mathcal{L}_{G,i}(t)$ will have at most two inflection points, indicating a necessary condition for epoch-wise double descent similar to the one given by corollary 1. With more relaxed assumptions, the error curve for the multi-layer dynamics might show more complex behaviour, potentially with additional, unidentified factors causing epoch-wise double descent in deeper models.

The effect of coupling In the decoupled dynamics, eq. (6), the weights in both the first and second layer of the two-layer network are each connected only to a single set of eigenvalue λ_i and singular value σ_i . If dynamics are not decoupled, however, weights can be connected to several eigenvalues of the input covariance matrix as well as several singular values of the input-output covariance matrix, resulting in interaction between weights in the learning dynamics, see e.g. [34, 2]. We might expect such an interaction to give rise to new types of epoch-wise double descent behaviours. For example, in [22] it is hypothesised that epoch-wise double descent in two-layer neural networks with ReLU activation emerges because the weights in the second layer are learnt faster than the first layer weights. This could indicate a trade-off between independent evolution of weights and evolution through interaction. While not observed for the decoupled two-layer dynamics, it remains to be investigated if such a behaviour could also be observed in the (coupled) linear two-layer neural network.

Acknowledgements

This research is financially supported by the Swedish Research Council, the Wallenberg AI, Autonomous Systems and Software Program (WASP) funded by the Knut and Alice Wallenberg Foundation, and the Excellence Center at Linköping–Lund in Information Technology (ELLIIT).

References

- [1] B. Adlam and J. Pennington. Understanding Double Descent Requires a Fine-Grained Bias-Variance Decomposition. In *Advances in Neural Information Processing Systems*, 2020.
- [2] M. S. Advani, A. M. Saxe, and H. Sompolinsky. High-dimensional dynamics of generalization error in neural networks. *Neural Networks*, 132:428–446, 2020.
- [3] S. Arora, S. S. Du, W. Hu, Z. Li, and R. Wang. Fine-Grained Analysis of Optimization and Generalization for Overparameterized Two-Layer Neural Networks. In *International Conference on Machine Learning*, 2019.
- [4] A. Atanasov, B. Bordelon, and C. Pehlevan. Neural networks as kernel learners: the silent alignment effect. In *International Conference on Learning Representations*, 2022.
- [5] P. Baldi and Y. Chauvin. Temporal Evolution of Generalization during Learning in Linear Networks. *Neural Computation*, 3(4):589–603, 1991.
- [6] M. Belkin, D. Hsu, S. Ma, and S. Mandal. Reconciling modern machine-learning practice and the classical bias-variance tradeoff. *Proceedings of the National Academy of Sciences*, 116(32):15849–15854, 2019.
- [7] R. Berthier. Incremental Learning in Diagonal Linear Networks. *Journal of Machine Learning Research*, 24:1–26, 2023.
- [8] A. Bodin and N. Macris. Model, sample, and epoch-wise descents: exact solution of gradient flow in the random feature model. *Advances in Neural Information Processing Systems*, 2021.
- [9] A. Bodin and N. Macris. Gradient flow in the Gaussian covariate model: Exact solution of learning curves and multiple descent structures. *arXiv preprint arXiv:2212.06757*, 2022.
- [10] B. Bordelon and C. Pehlevan. Learning Curves for SGD on Structured Features. In *International Conference on Learning Representations*, 2022.
- [11] L. Braun, C. C. J. Dominé, J. E. Fitzgerald, and A. M. Saxe. Exact learning dynamics of deep linear networks with prior knowledge. In *Advances in Neural Information Processing Systems*, 2022.
- [12] N. S. Chatterji and P. M. Long. Deep Linear Networks can Benignly Overfit when Shallow Ones Do. *Journal of Machine Learning Research*, 24:1–39, 2023.
- [13] A. Curth, A. Jeffares, and M. van der Schaar. A U-turn on Double Descent: Rethinking Parameter Counting in Statistical Learning. In *Advances in Neural Information Processing Systems*, 2023.

- [14] S. D’Ascoli, L. Sagun, and G. Biroli. Triple Descent and the Two Kinds of Overfitting: Where & Why do they Appear? *Advances in Neural Information Processing Systems*, 2020.
- [15] M. Even, S. Pesme, S. Gunasekar, and N. Flammarion. (S) GD over Diagonal Linear Networks: Implicit Bias, Large Stepsizes and Edge of Stability. In *Advances in Neural Information Processing Systems*, 2023.
- [16] G. Gidel, F. Bach, and S. Lacoste-Julien. Implicit Regularization of Discrete Gradient Dynamics in Linear Neural Networks. *Advances in Neural Information Processing Systems*, 32, 2019.
- [17] D. Gissin, S. Shalev-Shwartz, and A. Daniely. The implicit bias of depth: How incremental learning drives generalization. In *International Conference on Learning Representations*, 2020.
- [18] S. Goldt, M. S. Advani, A. M. Saxe, F. Krzakala, and L. Zdeborová. Generalisation dynamics of online learning in over-parameterised neural networks. *arXiv preprint arXiv:1901.09085*, 2019.
- [19] S. Goldt, M. S. Advani, A. M. Saxe, F. Krzakala, and L. Zdeborová. Dynamics of stochastic gradient descent for two-layer neural networks in the teacher-student setup. *Journal of Statistical Mechanics: Theory and Experiment*, 2020(12):124010, 2020.
- [20] S. Goldt, M. Mézard, F. Krzakala, and L. Zdeborová. Modeling the Influence of Data Structure on Learning in Neural Networks: The Hidden Manifold Model. *Physical Review X*, 10(4):041044, 2020.
- [21] T. Hastie, A. Montanari, S. Rosset, and R. J. Tibshirani. Surprises in High-Dimensional Ridgeless Least Squares Interpolation. *The Annals of Statistics*, 50(2):949–986, 2022.
- [22] R. Heckel and F. F. Yilmaz. Early stopping in deep networks: double descent and how to eliminate it. In *International Conference on Learning Representations*, 2021.
- [23] D. Kunin, A. Raventós, C. Dominé, F. Chen, D. Klindt, A. Saxe, and S. Ganguli. Get rich quick: exact solutions reveal how unbalanced initializations promote rapid feature learning. *arXiv preprint arXiv:2406.06158*, 2024.
- [24] A. K. Lampinen and S. Ganguli. An analytic theory of generalization dynamics and transfer learning in deep linear networks. In *International Conference on Learning Representations*, pages 1–20, 2019.
- [25] J. Li, T. V. Nguyen, C. Hegde, and R. K. Wong. Implicit Sparse Regularization: The Impact of Depth and Early Stopping. In *Advances in Neural Information Processing Systems*, 2021.

- [26] J. Li, T. V. Nguyen, C. Hegde, and R. K. W. Wong. Implicit regularization for group sparsity. In *International Conference on Learning Representations*, 2023.
- [27] S. Mei, A. Montanari, and P.-M. Nguyen. A mean field view of the landscape of two-layer neural networks. *Proceedings of the National Academy of Sciences*, 115(33):E7665–E7671, 2018.
- [28] H. Min, S. Tarmouni, R. Vidal, and E. Mallada. On the Explicit Role of Initialization on the Convergence and Implicit Bias of Overparametrized Linear Networks. *International Conference on Machine Learning*, 2021.
- [29] H. Min, R. Vidal, and E. Mallada. On the Convergence of Gradient Flow on Multi-layer Linear Models. In *International Conference on Machine Learning*, 2023.
- [30] P. Nakkiran, G. Kaplun, Y. Bansal, T. Yang, B. Barak, and I. Sutskever. Deep double descent: Where bigger models and more data hurt. *Journal of Statistical Mechanics: Theory and Experiment*, 2021:124003, 2021.
- [31] S. Pesme and N. Flammarion. Saddle-to-Saddle Dynamics in Diagonal Linear Networks. In *Advances in Neural Information Processing Systems*, 2023.
- [32] S. Pesme, L. Pillaud-Vivien, and N. Flammarion. Implicit Bias of SGD for Diagonal Linear Networks: a Provable Benefit of Stochasticity. In *Advances in Neural Information Processing Systems*, 2021.
- [33] M. Pezeshki, A. Mitra, Y. Bengio, and G. Lajoie. Multi-scale Feature Learning Dynamics: Insights for Double Descent. In *International Conference on Machine Learning*, 2022.
- [34] A. M. Saxe, J. L. McClelland, and S. Ganguli. Exact solutions to the non-linear dynamics of learning in deep linear neural networks. In *International Conference on Learning Representations*, 2014.
- [35] A. M. Saxe, J. L. McClelland, and S. Ganguli. A mathematical theory of semantic development in deep neural networks. *Proceedings of the National Academy of Sciences of the United States of America*, 116(23):11537–11546, 2019.
- [36] C. Stephenson and T. Lee. When and how epochwise double descent happens. *arXiv preprint arXiv:2108.12006*, 2021.
- [37] S. Tarmouni, G. França, B. Haeffele, and R. Vidal. Understanding the Dynamics of Gradient Flow in Overparameterized Linear Models. In *International Conference on Machine Learning*, volume 139, pages 10153–10161, 2021.

- [38] Z. Wang and Y. Mao. On the generalization of models trained With SGD: Information-Theoretic Bounds and Implications. In *International Conference on Learning Representations*, 2022.
- [39] Z. Xu, H. Min, S. Tarmoun, E. Mallada, and R. Vidal. Linear Convergence of Gradient Descent for Finite Width Over-parametrized Linear Networks with General Initialization. In *International Conference on Artificial Intelligence and Statistics*, 2023.
- [40] C. Yun, S. Krishnan, and H. Mobahi. A unifying view on implicit bias in training linear neural networks. In *International Conference on Learning Representations*, 2021.

Supplementary material for *Towards understanding epoch-wise double descent in two-layer linear neural networks*

A Theoretical derivations

We provide derivations of the decoupled two-layer linear neural network dynamics as well as proofs for the main results of the paper. In the following derivations, we will use $A_{i,:}$ and $A_{:,i}$ to denote the i^{th} row and column, respectively, of a matrix A .

A.1 Decoupled dynamics for two-layer linear networks

To derive the decoupled dynamics eq. (5), we start from the MSE criterion in eq. (1). Using $n^{-1}Y^\top X = U^{(yx)}\Sigma V^{(yx)^\top}$ and $n^{-1}X^\top X = V\Lambda V^\top$, we have the following derivatives

$$\begin{aligned}\frac{d\mathcal{L}}{dW} &= \frac{1}{n}(Y^\top X - WX^\top X) = (U^{(yx)}\Sigma V^{(yx)^\top} - WV\Lambda V^\top), \\ \frac{d\mathcal{L}}{dW^{(1)}} &= W^{(2)^\top} \frac{d\mathcal{L}}{dW}, \\ \frac{d\mathcal{L}}{dW^{(2)}} &= \frac{d\mathcal{L}}{dW} W^{(1)^\top},\end{aligned}$$

yielding the dynamics

$$\begin{aligned}\frac{1}{\eta_a} \frac{d}{dt} W^{(1)} &= W^{(2)^\top} (U^{(yx)}\Sigma V^{(yx)^\top} - WV\Lambda V^\top), \\ \frac{1}{\eta_b} \frac{d}{dt} W^{(2)} &= (U^{(yx)}\Sigma V^{(yx)^\top} - WV\Lambda V^\top) W^{(1)^\top},\end{aligned}$$

with learning rates $\eta_a, \eta_b \geq 0$. Note that we do not yet assume $V = V^{(yx)}$, as is assumed in the main paper. We will introduce this assumption at a later stage in the derivations.

Following [34], we introduce the synaptic weights $Z := Z^{(2)}Z^{(1)}$ with $Z^{(1)} := W^{(1)}V^{(yx)}$, $Z^{(2)} := U^{(yx)^\top}W^{(2)}$. The dynamics for $Z^{(1)}$ are

$$\begin{aligned}\frac{1}{\eta_a} \frac{d}{dt} Z^{(1)} &= \frac{1}{\eta_a} \frac{d}{dt} W^{(1)}V^{(yx)} \\ &= W^{(2)^\top} (U^{(yx)}\Sigma V^{(yx)^\top} - WV\Lambda V^\top) V^{(yx)} \\ &= W^{(2)^\top} (U^{(yx)}\Sigma - U^{(yx)}ZV^{(yx)^\top}V\Lambda V^\top V^{(yx)}) \\ &= Z^{(2)^\top} (\Sigma - ZV^{(yx)^\top}V\Lambda V^\top V^{(yx)}).\end{aligned}$$

Similarly, the dynamics for $Z^{(2)}$ are

$$\begin{aligned}\frac{1}{\eta_b} \frac{d}{dt} Z^{(2)} &= \frac{1}{\eta_b} U^{(yx)\top} \frac{d}{dt} W^{(2)} \\ &= U^{(yx)\top} (U^{(yx)} \Sigma V^{(yx)\top} - WV\Lambda V^\top) W^{(1)\top} \\ &= (\Sigma - ZV^{(yx)\top} V\Lambda V^\top V^{(yx)}) Z^{(1)\top}.\end{aligned}$$

Let $V = [V_{:, \nu_1}^{(yx)}, V_{:, \nu_2}^{(yx)}, \dots, V_{:, \nu_{d_x}}^{(yx)}]$ for indices $\nu_1, \nu_2, \dots, \nu_{d_x} \in \{1, 2, \dots, d_x\}$, $\nu_i \neq \nu_j$ for $i \neq j$. In other words, V is equal to $V^{(yx)}$ but with permuted columns. Then, the $(i, j)^{\text{th}}$ element of $V^\top V^{(yx)}$ is

$$(V^\top V^{(yx)})_{i,j} = V_{:, \nu_i}^{(yx)} \cdot V_{:, j}^{(yx)} = \begin{cases} 1, & \text{if } \nu_i = j, \\ 0, & \text{otherwise,} \end{cases}$$

with \cdot the dot product.

Hence, the dynamics simplifies to

$$\begin{aligned}\frac{1}{\eta_a} \frac{d}{dt} Z^{(1)} &= Z^{(2)\top} (\Sigma - Z\tilde{\Lambda}), \\ \frac{1}{\eta_b} \frac{d}{dt} Z^{(2)} &= (\Sigma - Z\tilde{\Lambda}) Z^{(1)\top},\end{aligned}$$

where $\tilde{\Lambda}$ is Λ but with diagonal elements reshuffled, such that $\tilde{\Lambda}_{i,i} = \Lambda_{\nu_i, \nu_i}$.

Now, let $\alpha^{(i)}$ denote the i^{th} column of $Z^{(1)}$ and $\beta^{(i)\top}$ denote the i^{th} row of $Z^{(2)}$. Moreover, let $\tilde{\lambda}_i$ and σ_i be the i^{th} diagonal elements of $\tilde{\Lambda}$ and Σ , respectively. We derive the dynamics for $\alpha^{(i)}$, $i = 1, \dots, d_x$, and $\beta^{(i)}$, $i = 1, \dots, d_y$.

We note that Z has elements

$$Z_{i,j} = \alpha^{(j)} \cdot \beta^{(i)},$$

and therefore

$$(Z\tilde{\Lambda})_{i,j} = (\alpha^{(j)} \cdot \beta^{(i)}) \tilde{\lambda}_j.$$

Let $S := \Sigma - Z\tilde{\Lambda}$, with

$$S_{i,j} = \begin{cases} \sigma_i - (\alpha^{(i)} \cdot \beta^{(i)}) \tilde{\lambda}_i, & \text{if } j = i, \\ -(\alpha^{(j)} \cdot \beta^{(i)}) \tilde{\lambda}_j, & \text{otherwise.} \end{cases}$$

Then, for column $\alpha^{(i)}$,

$$(Z^{(2)\top} S)_{i,j} = \sum_k \beta_i^{(k)} S_{k,j},$$

and, hence,

$$\frac{1}{\eta_a} \frac{d}{dt} \alpha^{(i)} = \sum_j \beta^{(j)} S_{j,i} = (\sigma_i - \tilde{\lambda}_i(\alpha^{(i)} \cdot \beta^{(i)})) \beta^{(i)} - \tilde{\lambda}_i \sum_{j \neq i} (\alpha^{(i)} \cdot \beta^j) \beta^{(j)}.$$

For row $\beta^{(i)}$, note

$$(S Z^{(1)}{}^\top)_{i,j} = \sum_k S_{i,k} \alpha_j^{(k)}.$$

Therefore,

$$\frac{1}{\eta_b} \frac{d}{dt} \beta^{(i)} = \sum_j S_{i,j} \alpha^{(j)} = (\sigma_i - \tilde{\lambda}_i(\alpha^{(i)} \cdot \beta^{(i)})) \alpha^{(i)} - \sum_{j \neq i} \tilde{\lambda}_j(\alpha^{(j)} \cdot \beta^{(i)}) \alpha^{(j)}.$$

If we decouple modes by initialising $\alpha^{(i)}, \beta^{(i)} \propto r^{(i)}$, with $r^{(i)}$ constant, orthogonal unit vectors, where $r^{(i)} \cdot r^{(j)} = 0$ if $i \neq j$, we get

$$\begin{aligned} \frac{1}{\eta_a} \frac{d}{dt} \alpha^{(i)} &= (\sigma_i - \tilde{\lambda}_i(\alpha^{(i)} \cdot \beta^{(i)})) \beta^{(i)} \\ \frac{1}{\eta_b} \frac{d}{dt} \beta^{(i)} &= (\sigma_i - \tilde{\lambda}_i(\alpha^{(i)} \cdot \beta^{(i)})) \alpha^{(i)} \end{aligned}$$

We verify that, once decoupled, modes remain decoupled:

$$\begin{aligned} \frac{d}{dt} (\alpha^{(i)} \cdot \beta^j) &= \eta_a (\sigma_i - \tilde{\lambda}_i(\alpha^{(i)} \cdot \beta^{(i)})) \beta^{(i)} \cdot \beta^{(j)} \\ &\quad + \eta_b (\sigma_j - \tilde{\lambda}_j(\alpha^{(j)} \cdot \beta^{(j)})) \alpha^{(j)} \cdot \alpha^{(i)} \\ &= 0. \end{aligned}$$

We recover eq. (5), by rewriting the decoupled dynamics in terms of the scalar projections $a_i = \alpha^{(i)} \cdot r^{(i)}$ and $b_i = \beta^{(i)} \cdot r^{(i)}$

$$\begin{aligned} \frac{1}{\eta_a} \frac{da}{dt} &= \frac{1}{\eta_a} \frac{d}{dt} (\alpha^{(i)} \cdot r^{(i)}) = b_i (\sigma_i - \tilde{\lambda}_i a_i b_i), \\ \frac{1}{\eta_b} \frac{db}{dt} &= \frac{1}{\eta_b} \frac{d}{dt} (\beta^{(i)} \cdot r^{(i)}) = a_i (\sigma_i - \tilde{\lambda}_i a_i b_i). \end{aligned}$$

In addition, in the main paper, we assume $V = V^{(yx)}$ such that $\tilde{\Lambda} = \Lambda$. Then, replace $\tilde{\lambda}_i$ with λ_i , denoting the i^{th} diagonal element of Λ .

A.2 Deriving the bridged dynamics

We derive the solution eq. (6), starting with deriving the bridged dynamics in eq. (6) from eq. (5). In the following, as we only consider a single weight, we will drop all sub- and superscripts, i . Then, starting from eq. (6), let $z = \alpha \cdot \beta = ab$, for which

$$\frac{dz}{dt} = \frac{d}{dt} ab = (\eta_b a^2 + \eta_a b^2)(\sigma - \lambda z).$$

We note that

$$\frac{d}{dt}(\eta_b a^2 - \eta_a b^2) = 2\eta_b a \frac{da}{dt} - 2\eta_a b \frac{db}{dt} = 0.$$

Hence, $\eta_b a^2 - \eta_a b^2 = \gamma$ is constant. Therefore, we can rewrite

$$\frac{dz}{dt} = (\gamma + 2\eta_a b^2)(\sigma - \lambda z)$$

From the equality

$$z = ab = \pm \sqrt{\frac{(\gamma + \eta_a b^2)}{\eta_b}} b,$$

we find

$$b = \pm \sqrt{\frac{-\gamma \pm \sqrt{\gamma^2 + 4\eta_a \eta_b z^2}}{2\eta_a}}.$$

Note that only the plus sign in the square root gives a valid solution for general $\eta_a, \eta_b \geq 0, \gamma$. Hence, we have

$$b^2 = \frac{-\gamma + \sqrt{\gamma^2 + 4\eta_a \eta_b z^2}}{2\eta_a}.$$

Replacing b^2 in the current dynamics of z with this solution, we obtain

$$\frac{dz}{dt} = \sqrt{\gamma^2 + 4\eta^2 z^2}(\sigma - \lambda z), \quad (20)$$

with $\eta = \sqrt{\eta_a \eta_b}$.

A.3 Proof of proposition 1

For solving the differential equation, eq. (6), we focus on the case $z(0) < \sigma/\lambda$ with $\lambda > 0$. Note that eq. (6) is separable in z, t , and so

$$\int dt = \int \frac{dz}{\sqrt{\gamma^2 + 4\eta^2 z^2}(\sigma - \lambda z)},$$

again dropping the subscript i for notational clarity. Assuming $\lambda > 0$, we solve the integrals to find

$$t = \frac{\log \left(\frac{\sqrt{(\gamma^2 \lambda^2 + 4\eta^2 \sigma^2)(\gamma^2 + 4\eta^2 z^2)} + \gamma^2 \lambda + 4\eta^2 \sigma z}{\lambda(\sigma - \lambda z)} \right)}{\sqrt{\gamma^2 \lambda^2 + 4\eta^2 \sigma^2}} + C,$$

for a constant C . Note that we from here recover eq. (16), by plugging in $z = \bar{z} = (1 - \rho)z^*$.

Now, solving for $z = z(t)$, with initial value $z(0)$, we obtain

$$z(t) = \frac{C^2 \lambda^2 \sigma e^{2\sqrt{\gamma^2 \lambda^2 + 4\eta^2 \sigma^2} t} - 2C\gamma^2 \lambda^2 e^{\sqrt{\gamma^2 \lambda^2 + 4\eta^2 \sigma^2} t} - 4\gamma^2 \eta^2 \sigma}{\lambda \left(C^2 \lambda^2 e^{2\sqrt{\gamma^2 \lambda^2 + 4\eta^2 \sigma^2} t} + 8C\eta^2 \sigma e^{\sqrt{\gamma^2 \lambda^2 + 4\eta^2 \sigma^2} t} - 4\gamma^2 \eta^2 \right)},$$

with

$$C = \frac{\sqrt{(\gamma^2 \lambda^2 + 4\eta^2 \sigma^2)(\gamma^2 + 4\eta^2 z(0)^2)} + \gamma^2 \lambda + 4\eta^2 \sigma z(0)}{\lambda(\sigma - \lambda z(0))}.$$

Note that the solution to the dynamics, eq. (6), includes solving the equation

$$\begin{aligned} & \sqrt{(\gamma^2 \lambda^2 + 4\eta^2 \sigma^2)(\gamma^2 + 4\eta^2 z(0)^2)} \\ &= \lambda(\sigma - \lambda z(t)) C e^{\sqrt{\gamma^2 \lambda^2 + 4\eta^2 \sigma^2} t} - \gamma^2 \lambda - 4\eta^2 \sigma z(t), \end{aligned}$$

for which we require

$$\lambda(\sigma - \lambda z(t)) C e^{\sqrt{\gamma^2 \lambda^2 + 4\eta^2 \sigma^2} t} - \gamma^2 \lambda - 4\eta^2 \sigma z(t) \geq 0.$$

To verify if (and when) this holds, we rewrite the expression in terms of the solution $z(t)$, resulting in

$$\begin{aligned} & \lambda(\sigma - \lambda z(t)) C e^{\sqrt{\gamma^2 \lambda^2 + 4\eta^2 \sigma^2} t} - \gamma^2 \lambda - 4\eta^2 \sigma z(0) \\ &= \frac{(\gamma^2 \lambda^2 + 4\eta^2 \sigma^2)(C^2 \lambda^2 e^{2\sqrt{\gamma^2 \lambda^2 + 4\eta^2 \sigma^2} t} + 4\gamma^2 \eta^2)}{\lambda(C^2 \lambda^2 e^{2\sqrt{\gamma^2 \lambda^2 + 4\eta^2 \sigma^2} t} + 8C\eta^2 \sigma e^{\sqrt{\gamma^2 \lambda^2 + 4\eta^2 \sigma^2} t} - 4\gamma^2 \eta^2)}. \end{aligned}$$

We observe that the nominator is positive. For the denominator, note that if $z(0) < \sigma/\lambda$, then $C \geq 0$ and, therefore,

$$\begin{aligned} & \lambda(C^2 \lambda^2 e^{2\sqrt{\gamma^2 \lambda^2 + 4\eta^2 \sigma^2} t} + 8C\eta^2 \sigma e^{\sqrt{\gamma^2 \lambda^2 + 4\eta^2 \sigma^2} t} - 4\gamma^2 \eta^2) \\ & \geq \lambda(C^2 \lambda^2 + 8C\eta^2 \sigma - 4\gamma^2 \eta^2). \end{aligned}$$

Plugging in the expression for C , we find

$$\begin{aligned} & \lambda(C^2 \lambda^2 + 8C\eta^2 \sigma - 4\gamma^2 \eta^2) \\ &= \frac{2(\gamma^2 \lambda^2 + 4\eta^2 \sigma^2)}{\lambda^2(\sigma - \lambda z(0))^2} \\ & \quad \cdot \left(\sqrt{(\gamma^2 \lambda^2 + 4\eta^2 \sigma^2)(\gamma^2 + 4\eta^2 z(0)^2)} + \gamma^2 \lambda + 4\eta^2 \sigma z(0) \right). \end{aligned}$$

If $\gamma \neq 0$, and following the assumption that $\lambda > 0$, we conclude that this expression is positive. If $\gamma = 0$, we require $\eta > 0$ and $z(0) > 0$ for the expression

to be positive (otherwise it equals 0). Hence, the solution holds for $z(0) < \sigma/\lambda$ with $\lambda > 0$ if $\gamma \neq 0$ or, when $\gamma = 0$, if $\eta > 0$ and $z(0) > 0$. This finishes the proof of the first part of proposition 1. Before moving on to the next part of the proof, we point out that we recover eqs. (9) and (10), by inserting $\eta = 0$ and $\gamma = 0$, respectively, into the solution.

For the next part of proposition 1, we take the limit of the solution, $z(t)$, to find

$$\lim_{t \rightarrow \infty} z(t) = \begin{cases} \frac{\sigma}{\lambda}, & \text{if } \gamma \neq 0, \\ \frac{\sigma}{\lambda}, & \text{if } \gamma = 0, \eta, z(0) > 0, \\ z(0), & \text{if } \gamma = \eta = 0, \\ 0, & \text{otherwise.} \end{cases}$$

In addition, observe that, for large t , and assuming $\eta, z(0) > 0$ if $\gamma = 0$, we have

$$\begin{aligned} |z^* - z(t)| &= \left| \frac{2Ce^{\sqrt{\gamma^2\lambda^2+4\eta^2\sigma^2}t} (\gamma^2\lambda^2 + 4\eta^2\sigma^2)}{\lambda \left(C^2\lambda^2e^{2\sqrt{\gamma^2\lambda^2+4\eta^2\sigma^2}t} + 8C\eta^2\sigma e^{\sqrt{\gamma^2\lambda^2+4\eta^2\sigma^2}t} - 4\gamma^2\eta^2 \right)} \right| \\ &\simeq \left| 2C^{-1}\lambda^{-3}(\gamma^2\lambda^2 + 4\eta^2\sigma^2)e^{-\sqrt{\gamma^2\lambda^2+4\eta^2\sigma^2}t} \right|, \end{aligned}$$

with $|\cdot|$ denoting an absolute value and with $z^* = \sigma/\lambda$.

A.4 Proof of lemma 1 and proposition 2

We derive eq. (14), starting from

$$\mathcal{L}_G(t) = \frac{1}{2} \mathbb{E}_{x,y} \left[(y - xW(t)^\top)(y - xW(t)^\top)^\top \right],$$

with $x \sim \mathcal{N}(\mathbf{0}, \bar{\Lambda})$ and y defined in eq. (11).

First, we prove lemma 1, by rewriting the true weight matrix \bar{W} (eq. (11)) in terms of the global minimum. We have

$$Y^\top X (X^\top X)^\dagger = U^{(yx)} \Sigma \Lambda^\dagger V^\top,$$

where \dagger denotes the Moore-Penrose pseudoinverse. Observe that the global minimum can also be expressed using eq. (11) according to

$$\begin{aligned} Y^\top X (X^\top X)^\dagger &= (\bar{W} X^\top X + E^\top X)(X^\top X)^\dagger \\ &= (\bar{W} V \Lambda + n^{-1/2} E^\top U \Lambda^{1/2}) \Lambda^\dagger V^\top, \end{aligned}$$

with

$$E = \begin{bmatrix} -\epsilon_1 - \\ -\epsilon_2 - \\ \dots \\ -\epsilon_n - \end{bmatrix},$$

the matrix of residual vectors $\epsilon_i = y_i - x_i \bar{W}^\top$, for $i = 1, \dots, n$. Using the two equations for the global minimum, we find

$$\begin{aligned}\bar{W} &= U^{(yx)} (\Sigma - n^{-1/2} U^{(yx)} \top E^\top U \Lambda^{1/2}) \Lambda^\dagger V^\top \\ &= U^{(yx)} (\Sigma \Lambda^\dagger - \tilde{E}^\top (\Lambda^{1/2})^\dagger) V^\top,\end{aligned}$$

with $\tilde{E} := n^{-1/2} U^\top E U^{(yx)}$. Subsequently, following the relation $\bar{W} = U^{(yx)} \bar{Z} V^{(yx)\top}$, the true weights in the synaptic weight space are

$$\bar{Z} := U^{(yx)\top} \bar{W} V = \Sigma \Lambda^\dagger - \tilde{E}^\top (\Lambda^{1/2})^\dagger.$$

Letting $\tilde{\epsilon}_i$ denote the i^{th} element on the main diagonal of \tilde{E} and assuming $\lambda_i > 0$, the i^{th} diagonal element of \bar{Z} follows directly as

$$\bar{z}_i = \sigma_i \lambda_i^{-1} - \tilde{\epsilon}_i \lambda_i^{-1/2}.$$

This finishes the proof of lemma 1.

Now, in the synaptic weight space, using $x \sim \mathcal{N}(\mathbf{0}, \bar{\Lambda})$ and with y following eq. (11), we have

$$\begin{aligned}\mathcal{L}_G(Z(t)) &= \frac{1}{2} \mathbb{E}_{x,y} \left[(y - x(U^{(yx)} Z(t) V^\top)^\top) (y - x(U^{(yx)} Z(t) V^\top)^\top)^\top \right] \\ &= \frac{1}{2} \mathbb{E}_{x,y} \left[(xV(\bar{Z} - Z(t))^\top U^{(yx)\top} + \epsilon) (xV(\bar{Z} - Z(t))^\top U^{(yx)\top} + \epsilon)^\top \right] \\ &= \frac{1}{2} \mathbb{E}_{x,y} \left[xV(\bar{Z} - Z(t))^\top (\bar{Z} - Z(t)) V^\top x^\top \right. \\ &\quad \left. + 2xV(\bar{Z} - Z(t))^\top U^{(yx)\top} \epsilon^\top + \epsilon \epsilon^\top \right] \\ &= \frac{1}{2} \left(\mathbb{E}_{x,y} \left[xV(\bar{Z} - Z(t))^\top (\bar{Z} - Z(t)) V^\top x^\top \right] + \text{Tr}(\Lambda^{(\epsilon)}) \right) \\ &\stackrel{(1)}{=} \frac{1}{2} \left(\text{Tr}((\bar{Z} - Z(t))^\top (\bar{Z} - Z(t)) V^\top \bar{\Lambda} V) + \text{Tr}(\Lambda^{(\epsilon)}) \right) \\ &\stackrel{(2)}{\approx} \frac{1}{2} \left(\text{Tr}((\bar{Z} - Z(t))^\top (\bar{Z} - Z(t)) \Lambda) + \text{Tr}(\Lambda^{(\epsilon)}) \right) \\ &= \frac{1}{2} \left(\text{Tr}((\Sigma - \tilde{E}^\top (\Lambda^{1/2})^\dagger - Z(t))^\top \right. \\ &\quad \left. (\Sigma - \tilde{E}^\top (\Lambda^{1/2})^\dagger - Z(t)) \Lambda) + \text{Tr}(\Lambda^{(\epsilon)}) \right) \\ &= \frac{1}{2} \sum_{i \in S_A} \lambda_i (\sigma_i \lambda_i^{-1} - \tilde{\epsilon}_i \lambda_i^{-1/2} - z_i(t))^2 + \text{const.},\end{aligned}$$

resulting in eq. (14). In (1), we use $\mathbb{E}_x[x A x^\top] = \text{Tr}(A \bar{\Lambda})$, with the matrix A defined as $A = V(\bar{Z} - Z(t))^\top (\bar{Z} - Z(t)) V^\top$, together with the cyclic property of the trace, and in (2) we use the approximation $V \Lambda V^\top \approx \bar{\Lambda}$. The final

constant term includes the noise term $\text{Tr}(\Lambda^{(\epsilon)})$ as well as a possible constant error corresponding to constant entries in $Z(t)$, including non-diagonal elements for which corresponding entries in \bar{Z} are non-zero.

For the second part of the proof, consider an individual error curve in the sum of eq. (14), which has the form

$$\mathcal{L}_{\mathcal{G},i}(t) = \lambda_i(\sigma_i \lambda_i^{-1} - \tilde{\epsilon}_i \lambda_i^{-1/2} - z_i(t))^2,$$

with $i \in S_{\mathcal{A}}$. To show that this error curve is either monotonically decreasing, U-shaped, or monotonically increasing in t , we study the gradient

$$\frac{d}{dt} \mathcal{L}_{\mathcal{G},i}(t) = -2\lambda_i(\sigma_i \lambda_i^{-1} - \tilde{\epsilon}_i \lambda_i^{-1/2} - z_i(t)) \frac{dz_i(t)}{dt}.$$

Following the dynamics in eq. (6), the sign of $dz_i(t)/dt$ will be determined by the term $(\sigma_i - \lambda z_i(t))$ and hence on the initialisation. If $z_i(0) \leq z_i^*$, $z_i(t)$ will monotonically increase in t with

$$\frac{dz_i(t)}{dt} \geq 0, \forall t.$$

On the other hand, if $z_i(0) > z_i^*$, $z_i(t)$ will monotonically decrease in t with

$$\frac{dz_i(t)}{dt} \leq 0, \forall t.$$

With this in mind, observe that the gradient of the error curve $\mathcal{L}_{\mathcal{G},i}(t)$ will change signs only at one point. We see this by solving

$$\frac{d}{dt} \mathcal{L}_{\mathcal{G},i}(t) = 0.$$

While one solution to this equation is $dz_i(t)/dt = 0$, we note that the gradient will not change signs at this point. Indeed if $dz_i(t)/dt = 0$, $z_i(t)$ will remain at its current value, and so will $\mathcal{L}_{\mathcal{G},i}(t)$. The other solution is

$$z_i(t) = \sigma_i \lambda_i^{-1} - \tilde{\epsilon}_i \lambda_i^{-1/2},$$

and as $z_i(t)$ is either monotonically increasing or decreasing in t , this point will be passed only once during the course of learning.

Now, following eq. (6), $z_i(t)$ will either increase or decrease in t , depending on the initialisation, starting at $z_i(0)$ and ending at z_i^* . An exception can be seen in the special case $\gamma_i = 0$ and $z_i(0) \leq 0$, where the trajectory will stop at $z_i(t) = 0$ (see appendix A.2). We observe that if

$$\sigma_i \lambda_i^{-1} - \tilde{\epsilon}_i \lambda_i^{-1/2} \geq z_i^* \geq z_i(0),$$

or

$$z_i(0) > z_i^* \geq \sigma_i \lambda_i^{-1} - \tilde{\epsilon}_i \lambda_i^{-1/2},$$

then

$$\frac{d}{dt} \mathcal{L}_{\mathcal{G},i}(t) \leq 0 \quad \forall t,$$

and so the error curve is monotonically decreasing in t . If instead

$$z_i^* \geq z_i(0) \geq \sigma_i \lambda_i^{-1} - \tilde{\epsilon}_i \lambda_i^{-1/2},$$

or

$$\sigma_i \lambda_i^{-1} - \tilde{\epsilon}_i \lambda_i^{-1/2} \geq z_i(0) > z_i^*,$$

then,

$$\frac{d}{dt} \mathcal{L}_{\mathcal{G},i}(t) \geq 0 \quad \forall t,$$

and the error curve is monotonically increasing in t . Finally, if the point $\sigma_i \lambda_i^{-1} - \tilde{\epsilon}_i \lambda_i^{-1/2}$ lies on the path between $z_i(0)$ and the global minimum z_i^* (or alternatively, the fixed point $z_i(t) = 0$ if $\gamma_i = 0, z_i(t) \leq 0$), i.e. if

$$z_i^* > \sigma_i \lambda_i^{-1} - \tilde{\epsilon}_i \lambda_i^{-1/2} > z_i(0),$$

or

$$z_i(0) > \sigma_i \lambda_i^{-1} - \tilde{\epsilon}_i \lambda_i^{-1/2} > z_i^*,$$

the error curve $\mathcal{L}_{\mathcal{G},i}(t)$ will be decreasing in t up until the point $z_i(t) = \sigma_i \lambda_i^{-1} - \tilde{\epsilon}_i \lambda_i^{-1/2}$, after which the derivative of the error curve will change signs, and the error will become increasing in t . The resulting error curve hence will follow a U-shape. An exception can be seen for the case $\gamma_i = 0$ and $z(0) \leq 0$, where the trajectory might stop before the point $z_i(t) = \sigma_i \lambda_i^{-1} - \tilde{\epsilon}_i \lambda_i^{-1/2}$. In this case, the error curve will yet again be monotonically decreasing in t .

To conclude, each error curve $\mathcal{L}_{\mathcal{G},i}(t)$ as part of the sum in eq. (14), will be either monotonically decreasing, U-shaped, or monotonically increasing in t , and so the full generalisation curve is a sum of monotonically decreasing, U-shaped, or monotonically increasing curves, finishing the proof of proposition 2.

A.5 Proof of lemma 2

To prove lemma 2, we first note that, with $z(t)$ following eq. (6), the second derivative of $z(t)$ with respect to t is

$$\frac{d^2 z(t)}{dt^2} = 4\eta^2 z(t) (\sigma - \lambda z(t))^2 - \lambda (\gamma^2 + 4\eta^2 z(t)^2) (\sigma - \lambda z(t)),$$

dropping all subscripts i for notational clarity.

The first and second time derivatives of $\mathcal{L}_{\mathcal{G},i}(t)$ follow as

$$\begin{aligned}\frac{d}{dt}\mathcal{L}_{\mathcal{G},i}(t) &= -2\lambda(\bar{z} - z(t))\frac{dz(t)}{dt} \\ &= -2\lambda(\bar{z} - z(t))\sqrt{\gamma^2\lambda^2 + 4\eta^2\sigma^2}(\sigma - \lambda z(t)),\end{aligned}\quad (21)$$

$$\begin{aligned}\frac{d^2}{dt^2}\mathcal{L}_{\mathcal{G},i}(t) &= 2\lambda\left(\frac{dz(t)}{dt}\right)^2 - 2\lambda(\bar{z} - z(t))\frac{d^2z(t)}{dt^2} \\ &= 2\lambda(\sigma - \lambda z(t))\left((\gamma^2 + 4\eta^2z(t)^2)(\sigma + \lambda\bar{z} - 2\lambda z(t))\right. \\ &\quad \left.- 4\eta^2z(t)(\bar{z} - z(t))(\sigma - \lambda z(t))\right).\end{aligned}\quad (22)$$

Although we drop all other subscripts i , we keep the subscript on the loss function ($\mathcal{L}_{\mathcal{G},i}(t)$) to emphasise that we consider the error curve for a single weight $z(t)$.

Evaluated at $z(t) = \bar{z}$, the second derivative is

$$\frac{d^2}{dt^2}\mathcal{L}_{\mathcal{G},i}(t)\Big|_{z(t)=\bar{z}} = \frac{2\rho^2\sigma^2(\gamma^2\lambda^2 + 4\eta^2\sigma^2(1-\rho)^2)}{\lambda}, \quad (23)$$

replacing $\bar{z} = (1-\rho)\sigma/\lambda$. We immediately see that this derivative is positive if $1 \geq \rho > 0$, with an exception for the case $\rho = 1$ if $\gamma = 0$, but note that this scenario is not included under conditions (i)-(v).

For $\rho = 0$, to see that the curve is convex leading up to the point \bar{z} , note that solving

$$\frac{d^2}{dt^2}\mathcal{L}_{\mathcal{G},i}(t) = 0,$$

gives two potential inflection points

$$\hat{z}^\pm = \frac{\eta\sigma \pm \sqrt{\eta^2\sigma^2 - 6\gamma^2\lambda^2}}{6\lambda\eta}.$$

(the other solutions are undulation points). The roots \hat{z}^\pm are real if $\eta^2\sigma^2 \geq 6\gamma^2\lambda^2$ (including the case $\gamma = 0$). In this case, observe that we can upper bound the square root $\sqrt{\eta^2\sigma^2 - 6\gamma^2\lambda^2} \leq \eta\sigma$, and so

$$\hat{z}^\pm \leq \frac{\sigma}{3\lambda}.$$

Observe that this upper bound lies before the point $\bar{z} = z^*$. Evaluating the second curve at a point beyond the upper bound, we find

$$\frac{d^2}{dt^2}\mathcal{L}_{\mathcal{G},i}(t)\Big|_{z(t)=\frac{\sigma}{2\lambda}} = \gamma^2\lambda\sigma + \frac{\eta^2\sigma^4}{2\lambda} > 0,$$

with the inequality following from conditions (i)-(v). Hence, the curve is convex leading up to the minimum \bar{z} . If instead $\eta^2\sigma^2 < 6\gamma^2\lambda^2$ (including the case

$\eta = 0$), then the roots \hat{z}^\pm are complex, and so there are no inflection points in the error curve. As we have shown that the curve is convex at a point in the curve, the curve must be convex on the full path, and so, again, it must be convex leading up to the minimum. Since for $\rho = 0$, the true minimum \bar{z} is equal to the global minimum z^* , which is reached at $t \rightarrow \infty$, the error curve will gradually go towards 0 as $t \rightarrow \infty$. While the second derivative is 0 at \bar{z} if $\rho = 0$, see eq. (23), the error curve will not change convexity at this point, and hence, the minimum is an undulation point. This concludes the proof of lemma 2.

A.6 Proof of lemma 3

For proving lemma 3, we seek the inflection points of the error curve eq. (15), with $z(t)$ following eq. (6) and under assumptions (i)-(iv) introduced in the main paper. As in previous derivations, we will, for notational clarity, drop all subscripts i (with an exception for the subscript on the loss, $\mathcal{L}_{\mathcal{G},i}(t)$).

The first and second time derivatives of $\mathcal{L}_{\mathcal{G},i}(t)$ are given in eqs. (21) and (22). Before moving on to analysing the inflection points of the error curve, we evaluate its second derivative at the point $z(t) = 0$

$$\frac{d^2}{dt^2} \mathcal{L}_{\mathcal{G},i}(t) \Big|_{z(t)=0} = 2\gamma^2 \lambda \sigma^2 (2 - \rho).$$

We observe that under conditions (i)-(v), the second derivative is positive (or zero) at $z(t) = 0$.

For analysing the inflection points, we solve

$$\frac{d^2}{dt^2} \mathcal{L}_{\mathcal{G},i}(t) = 0,$$

with respect to $z(t)$, yielding

$$2(\sigma - \lambda z(t)) = 0,$$

or

$$\lambda((\gamma^2 + 4\eta^2 z(t)^2)(\sigma + \lambda \bar{z} - 2\lambda z(t)) - 4\eta^2 z(t)(\bar{z} - z(t))(\sigma - \lambda z(t))) = 0.$$

The solution to the first equation is $z(t) = z^*$. This is not an inflection point, but instead an undulation point, since $z(t)$ will not grow beyond its global minimum, and hence, the curve will not change convexity at this point. We instead continue by analysing the second equation, amounting to analysing the roots of the polynomial

$$\begin{aligned} f(z(t)) &= a_z z(t)^3 + b_z z(t)^2 + c_z z(t) + d_z, \\ a_z &= 12\lambda^2 \eta^2, \\ b_z &= -8\eta^2 \lambda \sigma (2 - \rho), \\ c_z &= 2(\gamma^2 \lambda^2 + 2\eta^2 \sigma^2 (1 - \rho)), \\ d_z &= -\gamma^2 \lambda \sigma (2 - \rho). \end{aligned}$$

We observe that the polynomial $f(z(t))$ with $\gamma \neq 0, \eta > 0$ is cubic in $z(t)$, and has a maximum of three real roots, possibly corresponding to inflection points in the error curve $\mathcal{L}_{G,i}(t)$. As there are no other possible inflection points, the error curve $\mathcal{L}_{G,i}(t)$ has a maximum of three inflection points on the interval $[0, z^*]$. This finishes the proof of the first part of lemma 3.

For analysing the relative positions of the potential inflection points of $\mathcal{L}_{G,i}(t)$, we will separate our further analysis into three cases: (i) $\gamma \neq 0, \eta > 0$, (ii) $\gamma \neq 0, \eta = 0$, (iii) $\gamma = 0, \eta > 0$.

Case $\gamma \neq 0, \eta > 0$. We start with the general case, assuming $\gamma \neq 0, \eta > 0$. We will carry out an analysis of the roots to the polynomial $f(z(t))$ with respect to the model weight $z(t)$, identifying the number of roots as well as their positions relative to the minimum \bar{z} . Note that, as $z(t)$ is continuous and growing in t under assumptions (i)-(iv), the analysis is directly translatable to the relative position and number of roots of the polynomial in t .

First, we observe that $f(z(t))$ has three distinct real roots if its discriminant

$$\begin{aligned}\Delta_f &= 18a_z b_z c_z d_z - 4a_z c_z^3 - 27a_z^2 d_z^2 + b_z^2 c_z^2 - 4b_z^3 d_z \\ &= -16\lambda^2 \eta^2 \left(24\gamma^6 \lambda^6 + \gamma^4 \lambda^4 \eta^2 \sigma^2 (11\rho^2 - 188\rho + 188) \right. \\ &\quad \left. + 16\gamma^2 \lambda^2 \eta^4 \sigma^4 (8\rho^4 - 33\rho^3 + 55\rho^2 - 44\rho + 22) \right. \\ &\quad \left. - 64\eta^6 \sigma^6 (\rho - 1)^2 (\rho^2 - \rho + 1) \right)\end{aligned}$$

is positive, i.e. $\Delta_f > 0$. If instead $\Delta_f = 0$, then at least two of the roots are the same. In the case $\Delta_f < 0$, the polynomial $f(z(t))$ has only one real root.

We will use *Rouths algorithm* to show that all roots of the polynomial have strictly positive real parts. For a cubic polynomial

$$a_0 x^3 + b_0 x^2 + a_1 + b_1,$$

Rouths algorithm analyses the following table

$$\begin{array}{cc} a_0 & a_1 \\ b_0 & b_1 \\ c_0 & 0 \\ d_0 & 0 \end{array}$$

with

$$\begin{aligned}c_0 &= \frac{b_0 a_1 - b_1 a_0}{b_0}, \\ d_0 &= b_1.\end{aligned}$$

From the table, Rouths theorem states that if $a_0 > 0$, then all roots of the polynomial has a strictly negative real part, if and only if the coefficients a_0, b_0, c_0, d_0 are strictly positive. The number of roots with strictly positive real parts is equal to the number of times that the sequence a_0, b_0, c_0, d_0 changes signs.

For the polynomial $f(z(t))$, we have

$$\begin{aligned} a_0 &= a_z = 12\lambda^2\eta^2, \\ b_0 &= b_z = -8\eta^2\lambda\sigma(2 - \rho), \\ c_0 &= \frac{b_z c_z - d_z a_z}{b_z} = \frac{\gamma^2\lambda^2}{2} + 4\eta^2\sigma^2(1 - \rho), \\ d_0 &= d_z = -\gamma^2\lambda\sigma(2 - \rho). \end{aligned}$$

We see directly that if $\gamma \neq 0, \eta > 0$ and under conditions (i)-(v), we have: $a_0 > 0, b_0 < 0, c_0 > 0, d_0 < 0$. Hence, the sequence a_0, b_0, c_0, d_0 changes signs three times, and, following Rouths theorem, the three roots of the polynomial all has strictly positive real parts. Hence, if the roots of $f(z(t))$ are real, they lie after the point $z(t) = 0$.

Note that, for $\gamma \neq 0, \eta > 0$, and under conditions (i)-(v), the error curve $\mathcal{L}_{G,i}(t)$ is convex at $z(t) = 0$ and $z(t) = \bar{z}$ (its second derivative is positive at these points), see eq. (23), with an exception for $\rho = 0$, where \bar{z} is instead an undulation point (see appendix A.5). For $1 \geq \rho > 0$, we hence must have an even number of inflection points on the interval $(0, \bar{z})$. In the case where $f(z(t))$ has one real root, $\Delta_f < 0$, this root, if corresponding to an inflection point, must therefore lie after the point \bar{z} . In this case, we would have zero inflection points on the interval $(0, \bar{z})$. However, if the polynomial has three distinct real roots, $\Delta_f > 0$, another possibility is that two, out of the three possible, inflection points lie on the interval $(0, \bar{z})$. For $\rho = 0$, we observe that one of the three possible roots of the polynomial $f(z(t))$ is equal to z^* , and $\mathcal{L}_{G,i}(t)$ has a maximum of two inflection points, one on the interval $(0, \bar{z})$ and one on the interval (\bar{z}, z^*) , see appendix A.5. We conclude, that for $\gamma \neq 0, \eta > 0$, a maximum of two inflection points lie in the interval $(0, \bar{z})$.

We investigate, in the case $\Delta_f > 0$, and for $1 \geq \rho > 0$ (we have already concluded that there is a maximum of two inflection points if $\rho = 0$), how many of the three roots of $f(z(t))$ lies in the interval $(0, \bar{z})$. For analysing the relative position of roots of $f(z(t))$ to the point \bar{z} , we shift the function $f(z(t))$ by \bar{z} , using a change of variables,

$$\begin{aligned} g(x(t)) &= a_x x(t)^3 + b_x x(t)^2 + c_x x(t) + d_x, \\ a_x &= 12\lambda^2\eta^2, \\ b_x &= -4\eta^2\lambda\sigma(7\rho - 5), \\ c_x &= 2(\gamma^2\lambda^2 + 2\eta^2\sigma^2(5\rho^2 - 7\rho + 2)), \\ d_x &= -\rho\sigma\left(\gamma^2\lambda + \frac{4\eta^2\sigma^2(1 - \rho)^2}{\lambda}\right), \end{aligned}$$

with $x(t) = z(t) - \bar{z}$, such that $g(0) = f(\bar{z})$. Note that $g(x(t))$ has equally many distinct roots in $x(t)$ as $f(z(t))$ has in $z(t)$, as shifting the function along the x-axis does not change this fact. Moreover, in the case $\Delta_f > 0$, with three real and distinct roots, since all roots of $f(z(t))$ are strictly positive, the roots of $g(x(t))$ must be larger than $-\bar{z}$.

We evaluate $g(x(t))$ at the points $x(t) = -\bar{z}$ (corresponding to $z(t) = 0$) and $x(t) = 0$ (corresponding to $z(t) = \bar{z}$)

$$g(-\bar{z}) = -\gamma^2 \lambda \sigma(2 - \rho),$$

$$g(0) = -\rho \sigma \left(\gamma^2 \lambda + \frac{4\eta^2 \sigma^2 (1 - \rho)^2}{\lambda} \right).$$

Hence, under conditions (i)-(v) and with $\gamma \neq 0, \eta > 0, 1 \geq \rho > 0$, we have $g(-\bar{z}), g(0) < 0$. Now, if we can find a point in the interval $(-\bar{z}, 0)$ such that $g(x(t)) > 0$, then we must conclude that there are at least two roots of $g(x(t))$ lying on the interval $(-\bar{z}, 0)$, and therefore two roots of $f(z(t))$, lying on the interval $(0, \bar{z})$.

For this purpose, observe that if $g(x(t))$ has three distinct real roots ($\Delta_f > 0$), then the polynomial must also have two distinct and real local optima, one local minimum and one local maximum lying in between the roots of the polynomial. The local optima are

$$x^\pm = \frac{2\eta\sigma(7\rho - 5) \pm \sqrt{4\eta^2\sigma^2(4\rho^2 - 7\rho + 7) - 18\gamma^2\lambda^2}}{18\eta\lambda}$$

For $\gamma \neq 0, \eta > 0$, we have $a_x > 0$, and, therefore $g(x(t)) \rightarrow -\infty$ if $x(t) \rightarrow -\infty$ and $g(x(t)) \rightarrow \infty$ if $x(t) \rightarrow \infty$, and so the local maximum must be located before the local minimum, i.e. the local maximum is the point

$$x^- = \frac{2\eta\sigma(7\rho - 5) - \sqrt{4\eta^2\sigma^2(4\rho^2 - 7\rho + 7) - 18\gamma^2\lambda^2}}{18\eta\lambda}.$$

Clearly, $x^- < 0$ if $5/7 > \rho > 0$. Note also that in the case of three real and distinct roots, the polynomial $g(x(t))$ must be positive at the local maximum, i.e. $g(x^-) > 0$. Since all of the roots of $g(x(t))$ are larger than $-\bar{z}$ and as $g(-\bar{z}) < 0$, we therefore also must have $x^- > -\bar{z}$. Hence, we have found a point at which $g(x(t)) > 0$ and that lie on the interval $(-\bar{z}, 0)$. Coming back to the original polynomial, $f(z(t))$, we conclude that if $f(z(t))$ has three real and distinct roots and if $5/7 > \rho > 0$, then at least two of them must lie in the interval $(0, \bar{z})$. Hence, if all of the three roots of $f(z(t))$ correspond to inflection points in the curve $\mathcal{L}_{G,i}(t)$, as we can have only a maximum of two roots on the interval $(0, \bar{z})$, then exactly two of these must lie in the interval $(0, \bar{z})$, and the third on the interval (\bar{z}, z^*) .

Case $\gamma \neq 0, \eta = 0$. For the one-layer model, $\eta = 0$, the polynomial $f(z(t))$ simplifies to

$$f(z(t)) = 2\gamma^2 \lambda^2 z(t) - \gamma^2 \lambda \sigma(2 - \rho).$$

Solving $f(z(t)) = 0$, we find

$$\hat{z} = \frac{\sigma(2 - \rho)}{2\lambda}.$$

Note that for $\rho = 0$, we have $\hat{z} = z^*$, and, as $z(t)$ never grows beyond its global minimum z^* , the error curve $\mathcal{L}_{\mathcal{G},i}(t)$ has no inflection points.

For $1 \geq \rho > 0$, it is easily verified that

$$1 > \frac{2 - \rho}{2} > 1 - \rho,$$

and therefore $\hat{z} \in (\bar{z}, z^*)$. Moreover, for $\eta = 0, \gamma, \rho > 0$ and under conditions (i)-(v), we have

$$\frac{d^2}{dt^2} \mathcal{L}_{\mathcal{G},i}(t) \Big|_{z(t)=\bar{z}} = 2\gamma^2 \lambda \sigma^2 \rho^2 > 0.$$

To show that we have a change of convexity at \hat{z} , we take a point lying on the interval (\hat{z}, z^*) and evaluate the second derivative of the error at that point:

$$\frac{d^2}{dt^2} \mathcal{L}_{\mathcal{G},i}(t) \Big|_{z(t)=\frac{\sigma(2-0.5\rho)}{2\lambda}} = -\frac{\gamma^2 \lambda \sigma^2 \rho^2}{4} < 0.$$

Hence, under conditions (i)-(v), the error curve $\mathcal{L}_{\mathcal{G},i}(t)$ is concave beyond the root \hat{z} , indicating that the point $\hat{z} \in (\bar{z}, z^*)$ is indeed an inflection point of $\mathcal{L}_{\mathcal{G},i}(t)$. In terms of t , initialising at $z(0)$, this inflection point, using eq. (16), is

$$t(\hat{z}) = \frac{\log\left(\frac{2(\sigma - \lambda z(0))}{\sigma \rho}\right)}{|\gamma| \lambda},$$

lying in the interval $(t^{(1-\rho)z^*}, \infty)$.

Case $\gamma = 0, \eta > 0$. For $\gamma = 0, \eta > 0$, corresponding to the balanced two-layer dynamics, note that the case $\rho = 1$ is not covered by conditions (i)-(v) and hence we carry out the following analysis for $1 > \rho \geq 0$. With $\gamma = 0$, the polynomial $f(z(t))$ simplifies to

$$f(z(t)) = z(t) \left(12\lambda^2 \eta^2 z(t)^2 - 8\eta^2 \lambda \sigma (2 - \rho) z(t) + 4\eta^2 \sigma^2 (1 - \rho) \right).$$

First, we note that the solution $\hat{z} = 0$ of $f(z(t)) = 0$ is not an inflection point, as $z(t) \geq 0$. To find potential inflection points, we instead solve

$$12\lambda^2 \eta^2 z(t)^2 - 8\eta^2 \lambda \sigma (2 - \rho) z(t) + 4\eta^2 \sigma^2 (1 - \rho) = 0,$$

with solutions

$$\hat{z}^\pm = \frac{\sigma(2 - \rho \pm \sqrt{\rho^2 - \rho + 1})}{3\lambda}.$$

For the first root, \hat{z}^- , and with $1 > \rho \geq 0$, we can verify

$$1 - \rho > \frac{2 - \rho - \sqrt{\rho^2 - \rho + 1}}{3} > 0,$$

and $\hat{z}^- \in (0, \bar{z})$ for $1 > \rho \geq 0$. For the second root, \hat{z}^+ , observe that $\hat{z}^+ = z^*$ for $\rho = 0$, and hence, \hat{z}^+ is not an inflection point for $\rho = 0$. For $1 \geq \rho > 0$, we find

$$1 > \frac{2 - \rho + \sqrt{\rho^2 - \rho + 1}}{3} > 1 - \rho,$$

and, hence, $\hat{z}^+ \in (\bar{z}, z^*)$ for $1 \geq \rho > 0$. To verify the convexity of $\mathcal{L}_{\mathcal{G},i}(t)$ between the roots \hat{z}^-, \hat{z}^+ , we take a point on the interval (\hat{z}^-, \hat{z}^+) and evaluate the second derivative at this point

$$\frac{d^2}{dt^2} \mathcal{L}_{\mathcal{G},i}(t) \Big|_{z(t)=\frac{\sigma(2-\rho)}{3\lambda}} = \frac{8\eta^2\sigma^4(\rho-2)(\rho+1)(\rho^2-\rho+1)}{27\lambda} > 0.$$

In other words, $\mathcal{L}_{\mathcal{G},i}(t)$ is convex in between the roots.

Moreover, we observe that the error curve is concave outside of the interval (\hat{z}^-, \hat{z}^+) . First consider the case $1 > \rho > 0$. We can use the upper bound $1 > \sqrt{1 - \rho + \rho^2}$ to find a point lying on the interval $(0, \hat{z}^-)$, for which the second derivative of $\mathcal{L}_{\mathcal{G},i}(t)$ is negative

$$\frac{d^2}{dt^2} \mathcal{L}_{\mathcal{G},i}(t) \Big|_{z(t)=\frac{\sigma(1-\rho)}{3\lambda}} = -\frac{8\eta^2\sigma^4\rho(1-\rho)^2(\rho+2)}{27\lambda} < 0.$$

Similarly, we find a point lying on the interval (\hat{z}^+, z^*) , for which

$$\frac{d^2}{dt^2} \mathcal{L}_{\mathcal{G},i}(t) \Big|_{z(t)=\frac{\sigma(3-\rho)}{3\lambda}} = -\frac{8\eta^2\sigma^4\rho^2(\rho-1)(\rho-3)}{27\lambda} < 0.$$

Hence with $\gamma = 0, \eta > 0$ and for $1 > \rho > 0$ and under conditions (i)-(v) (iv)-(iv), the error curve $\mathcal{L}_{\mathcal{G},i}(t)$ has two inflection points: $\hat{z}^- \in (0, \bar{z})$ and $\hat{z}^+ \in (\bar{z}, \infty)$.

For $\rho = 0$, we have only one root of $f(z(t))$ lying in the interval $(0, z^*)$:

$$\hat{z}^- = \frac{\sigma}{3\lambda}.$$

We have shown already that, for $\rho = 0$, the error curve $\mathcal{L}_{\mathcal{G},i}(t)$ is convex at a point in the interval (\hat{z}^-, z^*) (see the evaluation of the second derivative at $z(t) = \sigma(2 - \rho)/(3\lambda)$). To show that \hat{z}^- is an inflection point we additionally evaluate the second derivative of $\mathcal{L}_{\mathcal{G},i}(t)$ at a point in the interval $(0, \hat{z}^-)$:

$$\frac{d^2}{dt^2} \mathcal{L}_{\mathcal{G},i}(t) \Big|_{z(t)=\frac{\sigma}{4\lambda}} = -\frac{9\eta^2\sigma^4}{32\lambda} < 0.$$

Hence, with $\gamma = 0, \eta > 0$, and for $\rho = 0$, the error curve $\mathcal{L}_{\mathcal{G},i}(t)$ has one inflection point at $\hat{z}^- \in (0, \bar{z})$.

In terms of t , initialising at $z(0)$ the inflection points \hat{z}^\pm , using eq. (16), translates to

$$t(\hat{z}^\pm) = \frac{\log \left(\frac{(\sigma - \lambda z(0))(1 \pm \sqrt{\rho^2 - \rho + 1})}{\lambda \rho z(0)} \right)}{2\eta\sigma},$$

if $1 > \rho > 0$. If $\rho = 0$, we have

$$t(\hat{z}^-) = \frac{\log \left(\frac{\sigma - \lambda z(0)}{2\lambda z(0)} \right)}{2\eta\sigma}.$$

The inflection point $t(\hat{z}^-)$ will lie in the interval $(0, t^{(1-\rho)z^*})$ if $z(0) < \hat{z}^-$, and will otherwise either lie at 0 ($z(0) = \hat{z}^-$), corresponding to an undulation point and not an inflection point, or lie outside of the interval $(0, t^{(1-\rho)z^*})$ ($z(0) > \hat{z}^-$), for which the inflection point will not exist. Meanwhile, $t(\hat{z}^+)$ will lie in the interval $(t^{(1-\rho)z^*}, \infty)$.

In summary, we conclude that, under conditions (i)-(v), the error curve $\mathcal{L}_{\mathcal{G},i}(t)$ has a maximum of three inflection points, whereof a maximum of two lies in the interval $(0, \bar{z})$. If three inflection points exist and $5/7 > \rho > 0$, then two inflection points lie in the interval $(0, \bar{z})$ and one in the interval (\bar{z}, z^*) . Under conditions (i)-(v), we note that $z(t)$ is continuous as well as growing in time, t , and hence the conclusions are directly transferable to the corresponding inflection points in terms of t , replacing \bar{z} with $t(\bar{z}) = t^{(1-\rho)z^*}$ and z^* with $t(z^*) = \infty$. Indeed, we can have $z(0) > 0$, and it is therefore possible that there is a fewer number of inflection points on the time interval $(0, \infty)$ compared to the variable interval $(0, z^*)$. However, note that the conclusions still hold, referring to a maximum number of inflection points, or being contingent on having exactly three inflection points. With this, we end the proof of lemma 3.

A.7 Proof of proposition 3 and corollary 1

To prove proposition 3 and corollary 1, we consider the weight matrix $Z(t)$ with $|S_{\mathcal{A}}|$ active weights, following eq. (6). The total generalisation error, eq. (14), is a sum over $|S_{\mathcal{A}}|$ error curves. We show that, under conditions (i)-(v), a necessary condition for this generalisation error to exhibit a double descent pattern over the course of learning, is that we can find at least one inflection point, \hat{t} , belonging to either one of the $|S_{\mathcal{A}}|$ individual error curves, such that

$$\min\{t_i^{(1-\rho_i)z_i^*}; i \in S_{\mathcal{A}}\} < \hat{t} < \max\{t_i^{(1-\rho_i)z_i^*}; i \in S_{\mathcal{A}}\}.$$

We prove this necessary condition by showing that if there is no inflection point \hat{t} lying in the interval $(\min\{t_i^{(1-\rho_i)z_i^*}; i \in S_{\mathcal{A}}\}, \max\{t_i^{(1-\rho_i)z_i^*}; i \in S_{\mathcal{A}}\})$, then the error curve $\mathcal{L}_{\mathcal{G}}(t)$ does *not* exhibit a double descent pattern.

We first observe that double descent requires that the error curve $\mathcal{L}_{\mathcal{G}}(t)$ declines in t , i.e.

$$\frac{d}{dt} \mathcal{L}_{\mathcal{G}}(t) < 0,$$

at a time interval succeeding an interval for which $\mathcal{L}_{\mathcal{G}}(t)$ grows in t , i.e.

$$\frac{d}{dt} \mathcal{L}_{\mathcal{G}}(t) > 0.$$

We show that this is not possible if there is no \hat{t} lying in the interval $(\min\{t_i^{(1-\rho_i)z_i^*}; i \in S_{\mathcal{A}}\}, \max\{t_i^{(1-\rho_i)z_i^*}; i \in S_{\mathcal{A}}\})$.

First, observe that in the time interval $[0, \min\{t_i^{(1-\rho_i)z_i^*}; i \in S_{\mathcal{A}}\}]$, all individual error curves $\mathcal{L}_{\mathcal{G},i}(t)$, $i \in S_{\mathcal{A}}$, are decreasing or constant in t , i.e.

$$\frac{d}{dt} \mathcal{L}_{\mathcal{G},i}(t) \leq 0, \forall i \in S_{\mathcal{A}},$$

and so

$$\frac{d}{dt} \mathcal{L}_{\mathcal{G}}(t) \leq 0,$$

following eq. (14). In addition, in the interval $[\max\{t_i^{(1-\rho_i)z_i^*}; i \in S_{\mathcal{A}}\}, \infty)$, we have

$$\frac{d}{dt} \mathcal{L}_{\mathcal{G},i}(t) \geq 0, \forall i \in S_{\mathcal{A}},$$

and therefore

$$\frac{d}{dt} \mathcal{L}_{\mathcal{G}}(t) \geq 0.$$

To determine the behaviour of the generalisation error in between the two points $\min\{t_i^{(1-\rho_i)z_i^*}; i \in S_{\mathcal{A}}\}$ and $\max\{t_i^{(1-\rho_i)z_i^*}; i \in S_{\mathcal{A}}\}$, we observe that under conditions (i)-(v) and following lemma 2, each individual error curve $\mathcal{L}_{\mathcal{G},i}(t)$, $i \in S_{\mathcal{A}}$, for which $1 \geq \rho_i > 0$, is convex at \bar{z} . We point out that for $\rho_i = 1$, we have $\bar{z}_i = 0$, and hence, under conditions (i)-(v), $z_i(t)$ must begin at the point \bar{z} , so the error curve will be convex to start. For $\rho_i = 0$, again following lemma 2, the curve is convex leading up to the minimum, at which point the second derivative of $\mathcal{L}_{\mathcal{G},i}(t)$ is 0, and after which $z_i(t)$ will remain constant (note, however, that this happens at $t \rightarrow \infty$).

Taken together, if there is no inflection point \hat{t} , belonging to either one of the individual error curves $\mathcal{L}_{\mathcal{G},i}(t)$, $i \in S_{\mathcal{A}}$, and lying in the interval $(\min\{t_i^{(1-\rho_i)z_i^*}; i \in S_{\mathcal{A}}\}, \max\{t_i^{(1-\rho_i)z_i^*}; i \in S_{\mathcal{A}}\})$, then, on this interval, we must have

$$\frac{d^2}{dt^2} \mathcal{L}_{\mathcal{G},i}(t) \geq 0, \forall i \in S_{\mathcal{A}},$$

and, therefore,

$$\frac{d^2}{dt^2} \mathcal{L}_{\mathcal{G}}(t) \geq 0.$$

Now, assuming that there are no inflection points on the interval $(\min\{t_i^{(1-\rho_i)z_i^*}; i \in S_{\mathcal{A}}\}, \max\{t_i^{(1-\rho_i)z_i^*}; i \in S_{\mathcal{A}}\})$, take any time point t' for which

$$\frac{d}{dt} \mathcal{L}_{\mathcal{G}}(t) \Big|_{t=t'} > 0,$$

i.e., the error curve $\mathcal{L}_G(t)$ is growing at time t' . Note that, by the previous statements made regarding the first and second time derivatives of $\mathcal{L}_G(t)$, we must have $t' \in (\min\{t_i^{(1-\rho_i)z_i^*}; i \in S_{\mathcal{A}}\}, \infty)$. Then, take any other time point t'' such that $t'' > t'$. Either $t'' \in (\min\{t_i^{(1-\rho_i)z_i^*}; i \in S_{\mathcal{A}}\}, \max\{t_i^{(1-\rho_i)z_i^*}; i \in S_{\mathcal{A}}\})$, for which it must hold that, as $\mathcal{L}_G(t)$ is convex on the interval,

$$\frac{d}{dt}\mathcal{L}_G(t)\Big|_{t=t''} \geq \frac{d}{dt}\mathcal{L}_G(t)\Big|_{t=t'} > 0,$$

or $t'' \in [\max\{t_i^{(1-\rho_i)z_i^*}; i \in S_{\mathcal{A}}\}, \infty)$, for which

$$\frac{d}{dt}\mathcal{L}_G(t)\Big|_{t=t''} \geq 0.$$

We can conclude that there is no time point t'' , following a time point t' at which $\mathcal{L}_G(t)$ is growing in t , such that

$$\frac{d}{dt}\mathcal{L}_G(t)\Big|_{t=t''} < 0.$$

Therefore, the error curve $\mathcal{L}_G(t)$ will not exhibit a double descent pattern.

On the other hand, if there is an inflection point $\hat{t} \in (\min\{t_i^{(1-\rho_i)z_i^*}; i \in S_{\mathcal{A}}\}, \max\{t_i^{(1-\rho_i)z_i^*}; i \in S_{\mathcal{A}}\})$, belonging to either of the individual error curves $\mathcal{L}_{G,i}(t)$, $i \in S_{\mathcal{A}}$, there will be at least one sub-interval of $(\min\{t_i^{(1-\rho_i)z_i^*}; i \in S_{\mathcal{A}}\}, \max\{t_i^{(1-\rho_i)z_i^*}; i \in S_{\mathcal{A}}\})$, where it holds for at least one $z_i(t)$, $i \in S_{\mathcal{A}}$, that

$$\frac{d^2}{dt^2}\mathcal{L}_{G,i}(t) < 0.$$

Hence, the error curve $\mathcal{L}_G(t)$ possibly exhibits a non-convex behaviour on the interval $(\min\{t_i^{(1-\rho_i)z_i^*}; i \in S_{\mathcal{A}}\}, \max\{t_i^{(1-\rho_i)z_i^*}; i \in S_{\mathcal{A}}\})$, potentially giving rise to a double descent pattern. This concludes the proof of proposition 3.

For the proof of corollary 1, consider the special case with two active weights, $z_i(t), z_j(t)$. From the assumption $t_i^{(1-\rho_i)z_i^*} < t_j^{(1-\rho_j)z_j^*}$, it follows directly that

$$\begin{aligned} \min\{t_i^{(1-\rho_i)z_i^*}; i \in S_{\mathcal{A}}\} &= t_i^{(1-\rho_i)z_i^*}, \\ \max\{t_i^{(1-\rho_i)z_i^*}; i \in S_{\mathcal{A}}\} &= t_j^{(1-\rho_j)z_j^*}. \end{aligned}$$

Hence, the necessary condition for observing double descent simplifies to having at least one inflection point \hat{t} , belonging to either of the error curves $\mathcal{L}_{G,i}(t)$ and $\mathcal{L}_{G,j}(t)$, with

$$t_i^{(1-\rho_i)z_i^*} < \hat{t} < t_i^{(1-\rho_i)z_i^*}.$$

Now, provided that it exists, let \hat{t}_j^- denote the maximum inflection point belonging to the second curve, $\mathcal{L}_{G,j}(t)$, lying in the interval $(0, t_j^{(1-\rho_j)z_j^*})$. Moreover,

let, provided that it exists, \hat{t}_i^+ denote the minimum inflection point belonging to the first error curve, $\mathcal{L}_{G,i}(t)$, and lying on the interval $(t_i^{(1-\rho_i)z_i^*}, \infty)$. We note that we only need to consider the maximum inflection point on the interval $(0, t_j^{(1-\rho_j)z_j^*})$ belonging to the curve $\mathcal{L}_{G,j}(t)$, as if a smaller inflection point exists on the same interval and this inflection point also lies in the interval $(t_i^{(1-\rho_i)z_i^*}, t_j^{(1-\rho_j)z_j^*})$, so must \hat{t}_i^+ . In a similar manner, we only need to consider the minimum inflection point on the interval $(t_i^{(1-\rho_i)z_i^*}, \infty)$, belonging to the curve $\mathcal{L}_{G,i}(t)$, as if a larger inflection point exists on this interval and also lies in the interval $(t_i^{(1-\rho_i)z_i^*}, t_j^{(1-\rho_j)z_j^*})$, so must \hat{t}_i^+ . Then, a necessary condition for double descent, following the condition above, is that at least one of the two inflection points \hat{t}_i^+ and \hat{t}_j^- lies in the interval $(t_i^{(1-\rho_i)z_i^*}, t_j^{(1-\rho_j)z_j^*})$, which can be equivalently written as fulfilling one of

$$\begin{aligned} t_i^{(1-\rho_i)z_i^*} &< \hat{t}_j^-, \\ \hat{t}_i^+ &< t_i^{(1-\rho_i)z_i^*}. \end{aligned}$$

Note that assuming $t_i^{(1-\rho_i)z_i^*} < t_j^{(1-\rho_j)z_j^*}$ is without loss of generality. If the opposite holds, just change the order of $z_i(t)$ and $z_j(t)$. This concludes the proof of corollary 1.

A.8 Deep linear models

We derive the approximate dynamics of decoupled multi-layer linear neural networks, eq. (19), and identify inflection points in the error curve eq. (15) with $z_i(t)$ following the derived dynamics.

A.8.1 Derivation of dynamics

To derive the multi-layer dynamics in eq. (19), we start from the linear model of L layers

$$\begin{aligned} \hat{y} &= xW^\top, \\ W &= \prod_{\ell=1}^L W^{(\ell)}, \end{aligned}$$

with weight matrices $W^{(\ell)} \in \mathbb{R}^{h^{(\ell)} \times h^{(\ell-1)}}$, and where $h^{(0)} = d_x$ and $h^{(L)} = d_y$. Gradients of the MSE loss, eq. (1), are

$$\frac{1}{\eta_\ell} \frac{d}{dt} W^{(\ell)} = \frac{1}{n} \left(\prod_{j=\ell+1}^L W^{(j)} \right)^\top (Y^\top X - WX^\top X) \left(\prod_{j=1}^{\ell-1} W^{(j)} \right)^\top,$$

with $\eta_\ell \geq 0$ the learning rate of layer ℓ and where we assume $\prod_{j=\ell}^{\ell_u} W^{(j)} = \mathbb{I}$ (the identity matrix) if $\ell_l > \ell_u$.

We follow [34] and initialise weight matrices as $W^{(\ell)}(0) = R^{(\ell+1)} D^{(\ell)} R^{(\ell)\top}$, where $R^{(\ell)}$, for $\ell = 1, 2, \dots, L$, are orthogonal matrices, with $R^{(1)} = V$ and $R^{(L)} = U^{(yx)}$, and $D^{(\ell)}$, for $\ell = 1, 2, \dots, L$, are diagonal matrices. The synaptic weights $Z^{(\ell)} = R^{(\ell+1)\top} W^{(\ell)} R^{(\ell)}$, using the SVDs of X and $Y^\top X$ (as previously), then evolve as

$$\frac{1}{\eta_\ell} \frac{d}{dt} Z^{(\ell)} = \left(\prod_{j=\ell+1}^L Z^{(j)} \right)^\top (\Sigma - Z \Lambda) \left(\prod_{j=1}^{\ell-1} Z^{(j)} \right)^\top.$$

Observe that, with the given initialisation, $Z^{(\ell)}(0)$, $\ell = 1, 2, \dots, L$, is diagonal, and the gradients of any non-diagonal elements will be zero. Following this, each weight matrix $Z^{(\ell)}(t)$ will remain diagonal throughout the course of learning. The gradient of the i^{th} diagonal element of layer ℓ , denoted $a_i^{(\ell)}$, is

$$\frac{1}{\eta_\ell} \frac{da_i^{(\ell)}}{dt} = \prod_{j \neq \ell} a_i^{(j)} \left(\sigma_i - \lambda_i \prod_{j=1}^L a_i^{(j)} \right),$$

with λ_i and σ_i the i^{th} diagonal elements of Λ and Σ , respectively.

Similar to [34] and the two layer dynamics in eq. (5), these dynamics exhibit conserved quantities in the form of $\eta_j a_i^{(\ell)^2} - \eta_\ell a_i^{(j)^2} = \gamma_i^{(\ell,j)} \forall \ell, j \in \{1, \dots, L\}$. This, we can easily verify as

$$\frac{d}{dt} (\eta_j a_i^{(\ell)^2} - \eta_\ell a_i^{(j)^2}) = 2\eta_j a_i^{(\ell)} \frac{da_i^{(\ell)}}{dt} - 2\eta_\ell a_i^{(j)} \frac{da_i^{(j)}}{dt} = 0.$$

We use the conserved quantities to rewrite the gradient dynamics for the i^{th} diagonal element, $z_i = \prod_{j=1}^L a_i^{(j)}$, of the full weight matrix Z

$$\begin{aligned} \frac{dz_i}{dt} &= \sum_{j=1}^L \eta_j \prod_{k \neq j} a_i^{(k)^2} (\sigma_i - \lambda_i z_i) \\ &= \sum_{j=1}^L \eta_j \prod_{k \neq j} \frac{\gamma_i^{(k,L)} + \eta_k a_i^{(L)^2}}{\eta_L} (\sigma_i - \lambda_i z_i). \end{aligned}$$

To simplify the dynamics further, we assume L even, and group parameters in two groups, with $\gamma_i^{(j,L)} = \gamma_i$, $\eta_j = \eta_1$, for $j = 1, \dots, L/2$, and $\gamma_i^{(j,L)} = 0$, $\eta_j = \eta_L$, for $j = L/2 + 1, \dots, L$. Then,

$$z_i = \prod_{j=1}^L a_i^{(j)} = \pm \left(\sqrt{\frac{\gamma_i + \eta_1 a_i^{(L)^2}}{\eta_L}} \right)^{L/2} \left(\sqrt{a_i^{(L)^2}} \right)^{L/2},$$

from which we find

$$a_i^{(L)^2} = \frac{-\gamma_i + \sqrt{\gamma_i^2 + 4\eta_1 \eta_L z_i^{4/L}}}{2\eta_1}.$$

Inserting this into the dynamics of z_i and simplifying, we obtain

$$\frac{dz_i}{dt} = \frac{L}{2} \sqrt{\gamma_i^2 + 4\eta_1\eta_L z_i^{4/L}} z_i^{2(1-2/L)} (\sigma_i - \lambda_i z_i).$$

For large L , we have

$$\frac{dz_i}{dt} \approx \frac{L}{2} |\gamma_i| z_i^2 (\sigma_i - \lambda_i z_i),$$

recovering eq. (19).

A.8.2 Generalisation error

Assuming that the true model is linear, eq. (11), we note that we can rewrite the generalisation error of the multi-layer linear model, eq. (19), just as for the two-layer linear model, as a sum over individual error curves, eq. (14). To understand the behaviour of the generalisation error of the weight matrix $Z(t)$ with weights following the decoupled dynamics of eq. (19), we analyse the behaviour of the error curve in eq. (15), under conditions (i)-(v) and provided that $\gamma_i \neq 0$ and $z_i(0) \neq 0$. The two additional conditions are necessary for the weight $z_i(t)$ to be active, i.e. $i \in S_{\mathcal{A}}$.

We analyse the shape of the error curve given in eq. (15), by identifying its inflection points. From here on, we will, as previously, drop all subscripts i . First, from eq. (19), we have

$$\frac{d^2 z}{dt^2} = \frac{1}{2} L^2 \gamma^2 z^3 (\sigma - \lambda z) (\sigma - \frac{3}{2} \lambda z),$$

The first and second time derivatives of the error curve in eq. (15) with $z(t)$ following eq. (19) are

$$\begin{aligned} \frac{d\mathcal{L}_{\mathcal{G},i}(t)}{dt} &= -L|\gamma|z(t)^2 ((1-\rho)\sigma - \lambda z(t)) (\sigma - \lambda z(t)), \\ \frac{d^2\mathcal{L}_{\mathcal{G},i}(t)}{dt^2} &= -\frac{1}{2} L^2 \gamma^2 z(t)^3 (\sigma - \lambda z(t)) (4\lambda^2 z(t)^2 - 3\lambda\sigma(2-\rho)z(t) + 2\sigma^2(1-\rho)). \end{aligned}$$

We point out that with the active weight $z(t)$ growing in t , the error curve in eq. (15) will be either monotonically decreasing, U-shaped or monotonically increasing in t . We can see this by noting that under conditions (i)-(v) and with $\gamma \neq 0, z(0) \neq 0$,

$$(\sigma - \lambda z(t)) \geq 0, \forall t.$$

Therefore, the first time derivative of $\mathcal{L}_{\mathcal{G},i}(t)$ changes signs only at one point, namely at $z(t) = \bar{z}$. If $\bar{z} \geq z^*$ or $\bar{z} \leq z(0)$, this point is never passed, and the error curve $\mathcal{L}_{\mathcal{G},i}(t)$ is monotonically decreasing or increasing in t , respectively. If $z^* > \bar{z} > z(0)$, the point \bar{z} is passed once, and the error curve $\mathcal{L}_{\mathcal{G},i}(t)$ is U-shaped. Therefore, epoch-wise double descent in the decoupled multi-layer

model, if it appears, is a result of a superposition of monotonically decreasing, U-shaped or monotonically increasing curves.

Next, we find potential inflection points of the error curve $\mathcal{L}_{\mathcal{G},i}(t)$ by solving

$$\frac{d^2\mathcal{L}_{\mathcal{G},i}(t)}{dt^2} = 0.$$

Solutions to this equation include $z(t) = 0$ and $z(t) = z^*$, none of which are inflection points, as $z(t) \in [0, z^*]$. The other two solutions are

$$\hat{z}^\pm = \frac{\sigma(6 - 3\rho \pm \sqrt{9\rho^2 - 4\rho + 4})}{8\lambda}$$

We can verify, under conditions (i)-(v) and with $\gamma \neq 0, z(0) \neq 0$, that for $1 > \rho \geq 0$

$$1 - \rho > \frac{6 - 3\rho - \sqrt{9\rho^2 - 4\rho + 4}}{8} > 0,$$

and so $\hat{z}^- \in (0, \bar{z})$. We can also verify, for $1 > \rho > 0$ we have

$$1 > \frac{6 - 3\rho + \sqrt{9\rho^2 - 4\rho + 4}}{8} > 1 - \rho,$$

and so $\hat{z}^+ \in (\bar{z}, z^*)$. Note that we exclude the case $\rho = 1$, as it under conditions (i)-(v) would require $z(0) = 0$, contradicting the assumption $z(0) > 0$ and making the weight inactive. We evaluate the second derivative at a point in between the two roots

$$\begin{aligned} \frac{d^2}{dt^2}\mathcal{L}_{\mathcal{G},i}(t) \Big|_{z(t)=\frac{3(2-\rho)\sigma}{8\lambda}} &= -\frac{27L^2\gamma^2\sigma^6(\rho-2)^3(3\rho+2)(9\rho^2-4\rho+4)}{131072\lambda^3} \\ &> 0, \end{aligned}$$

finding that the error curve $\mathcal{L}_{\mathcal{G},i}(t)$ is convex in between the roots \hat{z}^- and \hat{z}^+ . For $1 > \rho \geq 0$, we evaluate the second derivative at a point in the interval $(0, \hat{z}^-)$

$$\frac{d^2}{dt^2}\mathcal{L}_{\mathcal{G},i}(t) \Big|_{z(t)=\frac{3(1-\rho)\sigma}{8\lambda}} = -\frac{27L^2\gamma^2\sigma^6(\rho-1)^4(3\rho+5)(9\rho+5)}{131072\lambda^3} < 0,$$

and, for $1 > \rho > 0$, at a point in the interval (\hat{z}^+, z^*)

$$\frac{d^2}{dt^2}\mathcal{L}_{\mathcal{G},i}(t) \Big|_{z(t)=\frac{(8-\rho)\sigma}{8\lambda}} = -\frac{L^2\gamma^2\sigma^6\rho^2(\rho-8)^3(5\rho-12)}{131072\lambda^3} < 0,$$

provided that our assumptions hold. Hence, we find that the curve changes convexity around the roots \hat{z}^\pm , and that they indeed are inflection points under the given restrictions on ρ , with $\hat{z}^- \in (0, \bar{z})$ if $1 > \rho \geq 0$ and $\hat{z}^+ \in (\bar{z}, z^*)$ if $1 > \rho > 0$. Note that under conditions (i)-(v) with $\gamma \neq 0$ and $z(0) \neq 0$, a weight

$z(t)$ following the dynamics eq. (19) will monotonically increase in t . Hence, the inflection points \hat{z}^\pm will correspond to unique time points \hat{t}^\pm , for t^- provided that $z(0) < \hat{z}^-$. To conclude, under conditions (i)-(v) with $\gamma \neq 0$ and $z(0) \neq 0$, if $z(0) < \hat{z}^-$ and $1 > \rho \geq 0$, the first inflection point, \hat{t}^- , will lie in the interval $(0, t^{(1-\rho)z^*})$. Moreover, if $1 > \rho > 0$, there will be a second inflection point, lying in the interval $(t^{(1-\rho)z^*}, \infty)$.